Distribution Agreement

In presenting this dissertation as a partial fulfillment of the requirements for an advanced degree from Emory University, I hereby grant to Emory University and its agents the non-exclusive license to archive, make accessible, and display my thesis or dissertation in whole or in part in all forms of media, now or hereafter known, including display on the world wide web. I understand that I may select some access restrictions as part of the online submission of this thesis or dissertation. I retain all ownership rights to the copyright of the thesis or dissertation. I also retain the right to use in future works (such as articles or books) all or part of this thesis or dissertation.

Signature:

Jia Meng	Date

Mutational Analysis of Non-essential Genes of Respiratory Syncytial Virus

By

Jia Meng
Doctor of Philosophy

Graduate Division of Biological and Biomedical Sciences
Microbiology and Molecular Genetics

Martin L. Moore, Ph.D.
Advisor

Larry J. Anderson, MD
Committee Member

Richard K. Plemper, Ph.D.
Committee Member

David A. Steinhauer, Ph.D.
Committee Member

John Steel, Ph.D.
Committee Member

Accepted:

Lisa A. Tedesco, Ph.D.
Dean of the James T. Laney School of Graduate Studies

Date

Mutational Analysis of Non-essential Genes of Respiratory Syncytial Virus

By

Jia Meng
M.Sc., California State University Los Angeles, 2010

Advisor: Martin L. Moore, Ph.D.

An abstract of
A dissertation submitted to the Faculty of the
James T. Laney School of Graduate Studies of Emory University
in partial fulfillment of the requirements or the degree of
Doctor of Philosophy
in
Graduate Division of Biological and Biomedical Sciences
Microbiology and Molecular Genetics
2015

ABSTRACT

MUTATIONAL ANALYSIS OF NON-ESSENTIAL GENES OF RESPIRATORY SYNCYTIAL VIRUS

By
Jia Meng

Respiratory syncytial virus (RSV) is the most important pathogen underlying acute lower respiratory tract infections in infants. Currently there are no vaccines or antivirals. Understanding the functions of RSV virulence genes should provide new insights into development of vaccines and antivirals.

Two non-structural genes of RSV (NS1 and NS2) suppress the host immune responses. Deletion of either or both NS genes generated virus that was either under-attenuated or over-attenuated for an effective and safe vaccine candidate for infants and young children. We used a codon deoptimization strategy to reduce the expression of NS genes based on human codon usage bias, resulting in dNSh virus. dNSh was attenuated in BEAS-2B and primary normal human bronchial epithelial cells cultured at air-liquid interface, but not in Vero or HEp-2 cells. In BALB/c mice, dNSh exhibited 10-fold lower viral load yet induced higher levels of RSV-neutralizing antibodies than the A2 non-deoptimized virus. Both viruses induced the same protection efficacy against challenge strains A/1997/12-35 and A2-line19F. Upon codon deoptimization, the NS target protein, STAT2, was degraded to a lesser extent than infection with non-deoptimized virus. dNSh induced less NF-κB activation, suggesting less pro-inflammatory potential. Serial passages in BEAS-2B did not generate nucleotide changes in the deoptimized regions.

RSV strain differences are an important factor in pathogenesis. The two surface glycoproteins, attachment protein G and fusion protein F, play major functions during infection. Previous studies indicated G protein was not required for infection, based on the fact that G-null virus still replicates efficiently in several cell-lines. We re-evaluated the functions of the G gene for a clinical isolate A2001/2-20 (2-20) in comparison to the lab strain A2. We generated recombinant viruses containing G and F or no G protein from either A2 (kRSV-A2G-A2F and kRSV-GstopA2F) or 2-20 strains (kRSV-2-20G-2-20F and kRSV-Gstop2-20F). We quantified the contribution of G to virus binding, entry kinetics, infectivity, and replication *in vitro*. Removal of 2-20 G from the virus had more deleterious effects than removal of A2 G in all the above processes. Overall, the 2-20 strain F had a higher dependence on its G protein than did the A2 strain.

MUTATIONAL ANALYSIS OF NON-ESSENTIAL GENES OF RESPIRATORY SYNCYTIAL VIRUS

By

Jia Meng
M.S., California State University, Los Angeles, 2010

Advisor: Martin L. Moore, Ph.D.

A dissertation submitted to the Faculty of the
James T. Laney School of Graduate Studies of Emory University
in partial fulfillment of the requirements for the degree of
Doctor of Philosophy
in
Graduate Division of Biological and Biomedical Science
Microbiology and Molecular Genetics
2015

ACKNOWLEDGEMENTS

First, I would like to express my deep appreciation for my advisor, Dr. Martin L. Moore for instilling in me the spirit and confidence of independent thinking and the tremendous amount of trust he has put into me to accomplish the projects. I also would like to say “thank you” to him for his patience with me as I was in frustration and meddling in the lab.

Without my dearest parents, Lili Dong and Fanzhe Meng, I could never think of completing my Ph.D. studies alone. You are the best parents in this world could possibly be, I believe. I have no doubt you two will always be there just for me even when I start to question myself. Thank you very very much for the unconditional understanding and support! I feel truly blessed for having you as my family!

I also want to express my gratitude to my dearest friends, Ken Wang and Yuan He. You are the people here in the US that takes care of me emotionally when my parents were not there. You have taught me to grow stronger as a person. We shared laughter and tears. Only you two can understand some of my struggles as we share so much in common and we all care about each other that much! We are not born as a family but we are very much like a family already!

Without all of you in my life, I cannot become a true Ph.D..

TABLE OF CONTENTS

CHAPTER 4

CHAPTER 1: INTRODUCTION – AN OVERVIEW OF RESPIRATORY SYNCYTIAL VIRUS BIOLOGY

1.1 RSV EPIDEMIOLOGY, CLASSIFICATION

Respiratory syncytial virus (RSV) is the leading cause of childhood severe acute lower respiratory tract illness (ALRI), which manifest as bronchiolitis and pneumonia. Based on a prospective study, the estimated annual burden due to severe RSV disease is about 125000 hospitalizations in the US, 3.4 million ALRI and at least 66000 deaths globally [1]. In the US, RSV causes most ALRI hospitalizations in young children < 1year old (2.3%-2.6%) [2, 3]. In the most recent multicenter prospective surveillance study for community-acquired pneumonia in young children requiring hospitalizations, RSV was the most commonly detected viral agent [4]. Despite being primarily recognized as an important pediatric pathogen, RSV also causes great amount of disease in the elderly and immunosuppressed individuals [5]. Risk factors for developing severe RSV disease include prematurity, chronic lung disease, congenital heart disease, and immunodeficiencies [6]. However, more than 80% of RSV-related deaths happen in children without such underlying risk factors [6].

RSV belongs to the *Paramyxoviridae* family, *Pneumovirus* genus. The *Paramyxoviridae* family also contains many other important human and animal pathogens, including measles virus, human parainfluenza virus, Nipahvirus, Hendravirus, Newcastle disease virus, and canine distemper virus. Viruses in this family all consist of a single stranded negative sense RNA genome encapsidated in a lipid envelope [7]. RSV has a single serotype with two antigenic subgroups A and B, which can co-circulate within the population in the same year [8].

1.2 RSV STRUCTURE

RSV encodes ten genes from which eleven proteins are translated. The virion consists of a lipid bilayer derived from the host cell with matrix protein (M) lying underneath it. When examined using cryo-EM, cell culture grown RSV displays pleomorphic structures, ranging from completely filamentous shapes to completely spherical shapes with varying intermediates [9]. The viral RNA is encapsidated by the nucleoprotein N in a left-handed helix form as other paramyxoviruses [9]. Between the RNP complex and the matrix layer lies the M2-1 protein, the transcription processivity factor [10]. Viral RNA genome is associated with proteins, the nucleoprotein (N), the phosphoprotein (P), the transcription factor M2-1, and the polymerase L, all of which form the functional RNA-dependent RNA polymerase (RdRp) [7].

Three glycoproteins are embedded in the viral envelope, namely the attachment protein G, the fusion protein F, and the small hydrophobic protein SH. The function for the SH protein has not been well studied for RSV and this protein is dispensable for *in vitro* growth, just like the G protein [11]. It has been shown using biochemical methods that SH can form a viroporin structure [12] and can antagonize apoptosis [13]. The G and F proteins are the major targets for virus neutralization. Both F and G proteins form oligomeric structures and are visualized as “spikes” projecting from the virion surface. Compared to the G protein, the F protein is more conserved in amino acid sequence across RSV strains, and it also shares some degrees of sequence similarity to other members of the *Paramyxoviridae* family [14].

The F protein of RSV is a type I trans-membrane protein with a N-terminal signal peptide which is removed during intracellular transport. Major functions of F include mediating the membrane fusion process between the virus and the host cell. F is synthesized as a 69-kD immature uncleaved form, F0, which is subsequently processed by the intracellular furin protease at two polybasic sites (106-109 and 131-136) during maturation to generate the F1 and F2 fragments. F1 and F2 are linked by two disulfide bonds to form the monomer of the fusion complexes [15-18]. F monomers form trimers on the virion surface and both the pre-fusion and post-fusion structures of the F trimer have been solved. During membrane fusion, dramatic structural rearrangements occur in the pre-fusion F structure to become the post-fusion F. Similar to other paramyxovirus fusion proteins, RSV F undergoes structural changes that expose the fusion peptide and insert it into the host cell membrane. Subsequently, the heptad repeat (HRA) region associates with the other heptad repeat region (HRB) as the protein folds back to form the stable six-helix bundle structure typical of the post-fusion F structure. The post-fusion F maintains most of the antibody binding sites present in pre-fusion F, except for the antigenic site Φ [19-21]. The trigger for F fusion for RSV is currently unknown. This fusion process does not require the G protein as the recombinant vesicular stomatitis virus expressing only RSV F can infect cells and mediate syncytia formation [22]. F protein has also been shown to mediate certain host cell binding activities since virus lacking both the G and SH proteins can still bind and infect cells, and peptides derived from F protein can inhibit virus binding and infectivity [23, 24]. Recently, nucleolin has been shown to be a host cell receptor for RSV infection and virus binding to nucleolin is mediated by the F protein [25]. Other possible receptors for RSV include intracellular

adhesion molecule-1 (ICAM-1), CX3CR1, and annexin II [26-28]. RSV F has also been shown to activate toll-like receptor 4 (TLR4), thus activating the nuclear factor kappa B- (NF-κB) pathway which drives the pro-inflammatory cytokine expression [29].

The G protein is a type II trans-membrane protein that is highly glycosylated, which leads to an increase of its molecular weight from 36-kD for the unglycosylated form to around 90-kD as seen in mature G [30]. The size and glycosylation pattern of the G protein depends on the cell line in which it is produced: about 80 to 100-kD in immortalized cell lines or up to 180-kD when produced from primary well-differentiated HAE culture [31]. When grown in Vero cell line, the majority of G is a truncated form of 55-kD (lacking the C terminus), leading to decreased infectivity of the resulting virus [32]. The major function of G is to mediate virus binding to glycosaminoglycans (GAGs) on the cell surface but its function can be partially substituted by the F protein. G protein of RSV shares no sequence homology with other paramyxovirus attachment proteins nor does it possess the hemagglutinin or neuraminidase activities. Sequence conservation of the G gene is the lowest among all RSV genes across different strains [7]. Although G protein has a high degree of sequence variation, it contains a central conserved region consisting of 13 amino acids, which overlap with 4 conserved cysteine residues. The 4 conserved cysteines are connected by two disulfide bonds to form the "cysteine noose" structure in the mature G protein. However, this central conserved cysteine noose region of G protein is not required for replication *in vitro* [33]. A heparin-binding domain (HBD; 184A→T198T in A strains and 183K→197K in B strains) has been identified but it is likely dispensable for virus replication *in vitro* as deletion of most of this domain did

not affect virus growth in cell lines [34, 35]. G also contains a CX3C chemokine fractalkine motif ($cysteine_{182}$ and $cysteine_{186}$ of the cysteine noose) and has been shown to impair the trafficking of CX3CR1+ cytotoxic cells into the lung [36]. G can also bind the CX3CR1, the receptor for fractalkine, and induce chemotaxis of leukocytes in a Boyden chamber experiment [28]. The central conserved region is flanked by two large hypervariable mucin-like domains that are highly glycosylated. The sequence of the second mucin-like domain on the C terminus is normally used to classify RSV strains. This second hypervariable domain is very flexible and can accommodate 24 amino acid insertions (seen for strain A) and 20 amino acid insertions (seen for strain B) at the same region, as found for some recently emerging RSV clinical isolates [37, 38]. The G protein is produced from infected cells both as a membrane-bound, full-length protein as well as a secreted shorter form due to translation initiation at the second methionine codon and subsequent proteolytic processing [39-41]. Similar to membrane-bound G, secreted G of RSV can still bind to cell surface GAGs although the functional significance during RSV infection is currently unknown [42]. Secreted G protein has been shown to function as an antigen decoy to impair antibody neutralization of the virus and to inhibit antibody-mediated antiviral effect of leukocytes [43, 44].

1.3 RSV LIFE CYCLE AND REVERSE GENETICS SYSTEM

Upon fusion of the virus envelope with the host cell membrane, the nucleocapsid containing viral genomic RNA is released into the cytoplasm along with the RdRp consisting of N, P, M2-1, and L [45-48]. The negative sense RSV genome is flanked by a leader (Le) and a trailer (Tr) at the 3' and 5' ends, respectively, which share sequence conservation in the first 36 nucleotides as a reflection of promoter function [49]. The first

11 nucleotides in the 3' Le sequence are required for both transcription and replication [50]. Transcription of the mRNA starts as the RdRp recognizes the first gene start (GS) signal of the 3' proximal gene. Each RSV gene open reading frame (ORF) is flanked by a GS and a gene end (GE) sequence that are relatively conserved. Transcription of each gene starts from the GS and ends at GE with certain rate of failure, producing a read-through mRNA encoding two ORFs. Because of this inefficient transcription stop, there is a transcriptional gradient with the genes more proximal to the 3' end being transcribed more abundantly than the more distal genes. The trigger for shifting from transcription to genome replication depends on the accumulation of M2-2 protein [51]. Several host factors have been identified to regulate replication/transcription of RSV, including eukaryotic elongation factor 1A (eEF1A) [52].

Infectious recombinant RSV can be generated using a reverse genetics system. In this system, the plasmid encoding the antigenome (positive sense RNA) is co-transfected with four helper plasmids each encoding a separate component of the RdRp (N, P, M2-1, and L) into the BSR-T7/5 cell line (BHK-21 cell line with constitutive expression of T7 polymerase) to drive the expression of the antigenome and the helper plasmids [48, 53, 54]. This system has proved to be of great importance for RSV live-attenuated vaccine development efforts and analyzing individual RSV gene functions [33, 35, 55-59].

1.4 RSV CELL CULTURE SYSTEM

In addition to the immortalized monolayer cells lines such as HEp-2, A549, BEAS-2B and Vero, more complicated, well-differentiated, primary human bronchial epithelial cell culture systems have been developed for studying RSV pathogenesis [60-63]. Because of their differentiated state and directional responses to pathogen invasion, this

new type of *in vitro* culture system is gaining popularity in studying host-pathogen interaction happening at the airway epithelial surface [64-67]. RSV exclusively infects and is released from the apical surface, and mostly targets the apical ciliated cells, but not goblet cells. Virus infection in the absence of the immune response can last for over a month without obvious cytopathic effect (CPE) [60-63]. One thing worthy of attention is that these primary airway epithelial culture systems prove to be more accurate for rating RSV attenuation levels, ensuring their importance in development of effective and safe RSV live-attenuated vaccine candidates, especially when the small animal models for RSV are lacking [63]. In terms of virus-host interaction, these primary differentiated culture systems prove to be better representative systems than commonly used immortalized cell lines, especially when analyzing clinical strains of RSV.

1.5 RSV STRAIN DIFFERENCES

Although RSV has only one serotype and two antigenic subgroups, strain variations within both subgroups during an annual infection have been documented, showing an annual pattern of replacing the predominant circulating strain/subgroup with a different one [68]. Recent studies focusing on clinical isolates of RSV suggest some differences between the clinical isolates and prototypic lab-adapted strains such as A2 and Long [69, 70]. Using a primary pediatric bronchial epithelial cell culture system, the clinical isolates showed differences from lab-adapted A2 strain in terms of CPE (syncytium formation and apoptosis of infected cells), infectivity, growth kinetics, and cytokine responses [62, 71, 72]. Strain-dependent differences in RSV pathogenesis can also be replicated in the BALB/c mouse model in terms of lung viral load, mucus induction, Th2 cytokine

responses and histopathology [73]. These findings underscore the importance of choice of RSV strains for studying pathogen-host interaction.

1.6 RSV AND THE HOST INNATE IMMUNITY

An effective innate immune response to any invading pathogen plays a critical role in determining the direction and effectiveness of subsequent adaptive responses and accompanying diseases and tissue damage. Initiation of innate immune responses depends on the recognition of the pathogen-associated molecular patterns (PAMPs) by the various pattern recognition receptors (PRRs), including toll-like receptors (TLR), RIG-I-like receptors (RLR), and NOD-like receptors (NLR). In infected airway epithelial cells, RIG-I is activated by viral dsRNA during the early phase of RSV infection, which subsequently induces TLR3 expression, mediating the later phase of the innate response [74]. RSV infection induces activation of several TLRs, including TLR-2, TLR-3, TLR-4 (with CD14), and TLR-6 [29, 75, 76]. TLR knock-out mice indicate a role for TLR2 and TLR6 in mediating cytokine response in macrophages, affecting early neutrophil recruitment into the lung, and DC activation during RSV infection [76]. TLR3 may detect the replication intermediate for RSV, dsRNA, and mediate the production of pro-inflammatory cytokines/chemokines from infected epithelial cells, although viral replication is not affected by TLR3 deficiency [75, 77]. TLR4 and CD14 have been shown to mediate the host immune response to RSV infection [29, 76]. TLR4 is a critical regulator in NF-κB activation during the early phase of RSV infection [78]. Interestingly, RSV infection has also been suggested to affect the TLR3 and TLR4 mediated responses to environmental stimuli such as dsRNA and LPS, respectively, by upregulating the surface expression of TLR3 and TLR4 on airway epithelium [79, 80]. RSV also targets

TLR3- and TLR7-mediated IFNα induction in plasmacytoid dendritic cells [81]. TLR3 or TLR7 deficiency does not affect viral replication, suggesting additional innate immune components in antiviral defense [75, 77, 82]. More recently, the adaptor protein downstream of RIG-I and MDA-5, IFNβ promoter stimulator (IPS-1, also known as MAVS/VISA/Cardif), is implicated in controlling viral clearance, the inflammatory cytokine profile, and lung pathology during RSV infection [83]. RSV is shown to suppress host innate immune responses, especially type I and type III interferon (IFN) induction and responses, although type II IFN pathway is also suggested as a target of NS1 and NS2. These effects are mostly mediated by the two non-structural genes (NS1 and NS2), thus making them one of the most important virulence genes for this virus [84-93]. Targets of NS1 and NS2 proteins include STAT2, IRF-3, IRF-7, RIG-I, TRAF-3, and IKKε [84, 85, 87, 88, 92]. Both NS proteins are also shown to inhibit apoptosis in infected cells to support viral growth [94]. Deletions of NS1 and/or NS2 gene(s) have been used to attenuate the virus for vaccine development [95-98] (more on this in *RSV VACCINES AND ANTIVIRALS* section below).

More recently, a new host innate immune function mediated by the ribosomal protein L13a has been reported to restrict RSV replication through specifically targeting translation of the matrix protein M [99].

1.7 RSV AND THE HOST ADAPTIVE IMMUNITY

RSV encodes several genes that modulate various aspects of the adaptive immune response. The NS1 and NS2 genes skew the CD4+ T cell response, shifting from a Th1 to

a Th2 profile, while inhibit cytotoxic CD8+ T cell responses [100-102]. Inhibition of T cell response is partly dependent on the inhibition of type I IFN pathway as described previously. The NS1 and NS2 genes also suppress human DC maturation in a synergistic way as deletion of both genes results in higher DC maturation than deletion of either gene [102].

RSV G protein also negatively modulates host adaptive immunity. Produced as a secreted form, it acts as an antigen decoy to counter the antiviral effect of neutralizing antibodies through modulating the inflammatory leukocytes responses, mostly macrophages and complement system [43, 44]. The highly conserved central region of RSV G protein shares sequence homology with the CX3C chemokine fractalkine, can mimic fractalkine functions, and in BALB/c mouse mode, inhibit the cytotoxic T cell trafficking to the lung through this functional mimicry [28, 36]. Blocking the G protein CX3C-CX3CR1 interaction can reduce lung inflammation upon RSV infection [103]. The G protein CX3C motif also affects the human airway epithelial cell response and subsequent adaptive immune response profile [104].

Another RSV protein, nucleoprotein N, is shown to inhibit the formation of immunological synapse and inhibit subsequent T cell activation [105].

1.8 RSV VACCINES AND ANTIVIRALS

Direct medical cost due to severe RSV infection in the young children in the US alone was estimated to be around $652 million in 2000 [106]. A number of strategies

have been explored for development of effective and safe RSV vaccines. These include vectored vaccine containing either or both F and G protein, live-attenuated vaccines, subunit vaccines, and novel adjuvant vaccines (reviewed in [107, 108]). Inactivated whole virus approach has been avoided because of the history of formalin-inactivated RSV (FI-RSV) causing vaccine-associated enhanced disease upon natural infection in the 1960s [109]. Currently, the live-attenuated vaccine is the most clinically advanced for the pediatric population ([110] and reviewed in [107]).

Live-attenuated RSV vaccines have been experimentally proven to be safe for the young children population through surveillance studies and are not associated with vaccine-enhanced disease as seen with FI-RSV and some other inactivated and subunit RSV vaccines [110, 111]. Studies on the mechanisms of the FI-RSV failure identified effective RSV-neutralizing antibody of high avidity as a key factor for safe immunization of infants [112]. Traditional methods of attenuating RSV include serial passages under non-permissive temperature, chemical mutagenesis, and gene deletions/substitutions using reverse genetics. Despite the acclaimed safety profile in comparison to inactivated vaccine, live-attenuated vaccines also face the problems of phenotypic/genotypic reversion towards wild-type virulence (as seen with the most recent clinical trial of live-attenuated RSV vaccine candidate MEDI-559), and the difficulty of balancing attenuation and immunogenicity [95, 110, 113].

Present treatment options for infants hospitalized with severe RSV LRTI are primarily supportive (maintaining adequate levels of oxygenation, ventillatory support,

hydration with administration of intravenous fluids). Although bronchodilators and beta-adrenergic agents have been used in some patients to relieve the wheezing and increased bronchiolar smooth muscle constriction, their effectiveness in preventing hospitalization and other long-term benefits are not obviously favorable to argue for routine use. Although corticosteroids (to suppress the inflammatory responses) are also frequently used in the management of acute RSV LRTIs, there is not sufficient clinical data supporting their routine use in clinics. Ribavirin, a non-specific antiviral drug, is the only antiviral agent approved for treatment of acute RSV LRTIs. It is a guanosine analog that can interfere with virus replication. The clinical benefits of ribavirin are only marginal compared to its high costs and toxicity, thus its use is limited to patients with high risk factors [114]. Palivizumab, a humanized monoclonal antibody against the F protein, is currently the only FDA-approved specific prophylaxis agent for infants at high risk for developing severe RSV LRTIs. It has demonstrated significant benefits in reducing RSV hospitalizations in premature infants with underlying risk factors (chronic lung disease, prematurity, congenital heart disease, immune-deficiency) and safety profile [115]. But its high cost (US$6000-7000 per child) has limited its use to only a small subset of infants with severe RSV disease [116]. Recently, two RSV-specific antiviral drugs began clinical trials, ALS-8176 (NCT02202356) and GS-5086 (NCT02254421, NCT02254408). Other novel antiviral modalities are also explored, such as RNA-interference based agents.

CHAPTER 2

Refining the balance of attenuation and immunogenicity of respiratory syncytial virus by targeted codon deoptimization of virulence genes

The work of this chapter was published in September, 2014 in the MBio

Full article citation:

Meng J, Lee S, Hotard AL, Moore ML. 2014. Refining the balance of attenuation and immunogenicity of respiratory syncytial virus by targeted codon deoptimization of virulence genes. mBio 5(5):e01704-14.doi:10.1128/mBio.01704-14

Refining the balance of attenuation and immunogenicity of respiratory syncytial virus by targeted codon deoptimization of virulence genes

Jia Meng[a,b], Sujin Lee[a,b], Anne L. Hotard[a,b], Martin L. Moore[a,b]

[a]Department of Pediatrics, Emory University School of Medicine, Atlanta, Georgia, USA

[b]Children's Healthcare of Atlanta, Atlanta, Georgia, USA

Address correspondence to Martin L. Moore, martin.moore@emory.edu

ABSTRACT

Respiratory syncytial virus (RSV) is the most important pathogen for lower respiratory tract illness in children for which there is no licensed vaccine. Live-attenuated RSV vaccines are the most clinically advanced in children, but achieving an optimal balance of attenuation and immunogenicity is challenging. One way to potentially retain or enhance immunogenicity of attenuated virus is to mutate virulence genes that suppress host immune responses. The NS1 and NS2 virulence genes of the RSV A2 strain were codon deoptimized according to either human or virus codon usage bias, and the resulting recombinant viruses (dNSh and dNSv, respectively) were rescued by reverse genetics. RSV dNSh exhibited the desired phenotype of reduced NS1 and NS2 expression. RSV dNSh was attenuated in BEAS-2B and primary differentiated airway epithelial cells but not in HEp-2 or Vero cells. In BALB/c mice, RSV dNSh exhibited a lower viral load than did A2, and yet it induced slightly higher levels of RSV-neutralizing antibodies than did A2. RSV A2 and RSV dNSh induced equivalent protection against challenge strains A/1997/12-35 and A2-line19F. RSV dNSh caused less STAT2 degradation and less NF-κB activation than did A2 *in vitro*. Serial passage of RSV dNSh in BEAS-2B cells did not result in mutations in the deoptimized sequences. Taken together, RSV dNSh was moderately attenuated, more immunogenic, and equally protective compared to wild-type RSV and genetically stable.

IMPORTANCE

Respiratory syncytial virus (RSV) is the leading cause of infant viral death in the United States and worldwide, and no vaccine is available. Live-attenuated RSV vaccines are the most studied in children but have suffered from genetic instability and low immunogenicity. In order to address both obstacles, we selectively changed the codon usage of the RSV nonstructural (NS) virulence genes NS1 and NS2 to the least-used codons in the human genome (deoptimization). Compared to parental RSV, the codon deoptimized NS1/NS2 RSV was attenuated *in vitro* and in mice but induced higher levels of neutralizing antibodies and equivalent protection against challenge. We identified a new attenuating module that retains immunogenicity and is genetically stable, achieved through specific targeting of nonessential virulence genes by codon usage deoptimization.

INTRODUCTION

Respiratory syncytial virus (RSV) is the leading cause of lower respiratory tract illness (LRTI) in young children, manifested as bronchiolitis and pneumonia. In the Unites States, there are 132,000 to 172,000 estimated annual RSV-associated hospitalizations in children less than 5 years of age, with the highest hospitalization rates seen in very young infants [2]. RSV-associated LRTI results in an annual 66,000 to 199,000 deaths in children younger than 5 years old globally [1]. Prophylaxis currently available to prevent RSV-associated disease is a humanized monoclonal antibody (palivizumab) targeting the RSV fusion (F) protein, but it is prescribed only to infants with certain risk factors (prematurity, congenital heart disease, and congenital pulmonary dysplasia) [117], underscoring its limited use. Developing safe and effective vaccines against RSV faces many challenges (reviewed in references [118] and [119]).

RSV is a member of the *Paramyxovirdae* family, which contains important human pathogens. RSV carries 10 genes from which 11 proteins are produces, Two promoter-proximal non-structural (NS1 and NS2) proteins inhibit interferon (IFN) pathways, including type I and type III and potentially type II IFN [84-92]. NS1 and NS2 exert their immune-suppressive functions on human dendritic cells (DC) as well as $CD4^+$ and $CD8^+$ T cells [100-102]. NS1 and NS2 have also been shown to inhibit apoptosis in infected cells to facilitate viral growth [94]. Deletion of either NS1 or NS2 results in virus attenuation, while simultaneously deleting both NS1 and NS2 overattenuates the virus for vaccine purposes [95-98]. Combined with other attenuating cold-passage (*cp*) and/or temperature-sensitive (*ts*) point mutations, viruses with ΔNS1 or ΔNS2 were evaluated as

potential live-attenuated vaccine candidates, and ΔNS1 was highly attenuated, whereas ΔNS2 was underattenuated [95, 96, 120, 121]. Deletion of nonessential virulence genes provides a limited range of attenuation. Another challenge associated with setting the attenuation level of live-attenuated vaccines containing *cpts* point mutations is reversion or compensatory mutations. This is especially the case for RNA viruses [110, 120, 122], highlighting the need to further stabilize vaccine candidates. Attenuating mutations can also be associated with loss of immunogenicity due to reduced replicative fitness, as seen with RSV rA2ΔM2-2 [95, 123].

The codon usage deoptimization strategy was first used to address the problem of genetic instability of live-attenuated poliovirus vaccines [124, 125]. Codon deoptimization of the poliovirus capsid gene by incorporation of the rarest codons in the human genome reduced translation of capsid protein, resulting in virus attenuation [124, 125]. Another attenuation strategy, codon pair deoptimization, has been used to recode viral genes using rare codon pairs, which does not necessarily alter codon usage [126]. In this study, we applied codon usage deoptimization combined with selective targeting of viral immune-suppressive genes to a human pathogen and characterized the genetic stability, replicative fitness, immunogenicity, and protective efficacy of the recoded virus. To our knowledge, this is the first example of virus attenuation by codon deoptimization specifically of nonessential virulence genes. Our results demonstrate that targeting RSV NS1 and NS2 by codon deoptimization can be an effective strategy for developing live-attenuated vaccines with controllable attenuation, wild-type replication in Vero cells, genetic stability, and improved immunogenicity.

RESULTS

Generation of codon-deoptimized NS1 and NS2 RSV

We compared codon usage in the NS1 and NS2 genes of several RSV strains to the codon usage bias of the human genome [127]. Of the 18 amino acids used in the RSV NS1 and NS2 genes, 6 (33%) share the same least-used codons as those of human genes. Therefore, because we could not rule out the possibility that RSV utilizes a unique codon usage bias, we designed two mutant viruses with codon deoptimized NS1 and NS2 genes, namely, dNSh (wherein every codon in NS1 and NS2 is the least used for that amino acid in humans) and dNSv (all NS1 and NS2 codons are the least used by RSV). The dNSh design included 84 silent mutations in NS1 and 82 in NS2, the dNSv design included 145 silent mutations for NS1 and 103 mutations for NS2, and these nucleotide changes were distributed across the coding regions for both genes (Fig. 1). Wild-type NS1 and NS2 genes were replaced by deoptimized NS1 and NS2 genes using MscI and EcoRV sites (Fig. 2). The kRSV-dNSh and kRSV-dNSv mutants (k designates inclusion of the far-red fluorescent protein mKate2 in the first gene position, as described previously [53]) were rescued by reverse genetics, and the sequences of NS1 and NS2 genes were confirmed for all viral stocks. To test the genetic stability of the human codon deoptimized virus, we serially passaged the virus in three separate lines in BEAS-2B cells at 37°C for 10 passages and sequenced the final passage stocks (P10). All three P10 lines maintained the original deoptimized sequences for both NS1 and NS2 genes.

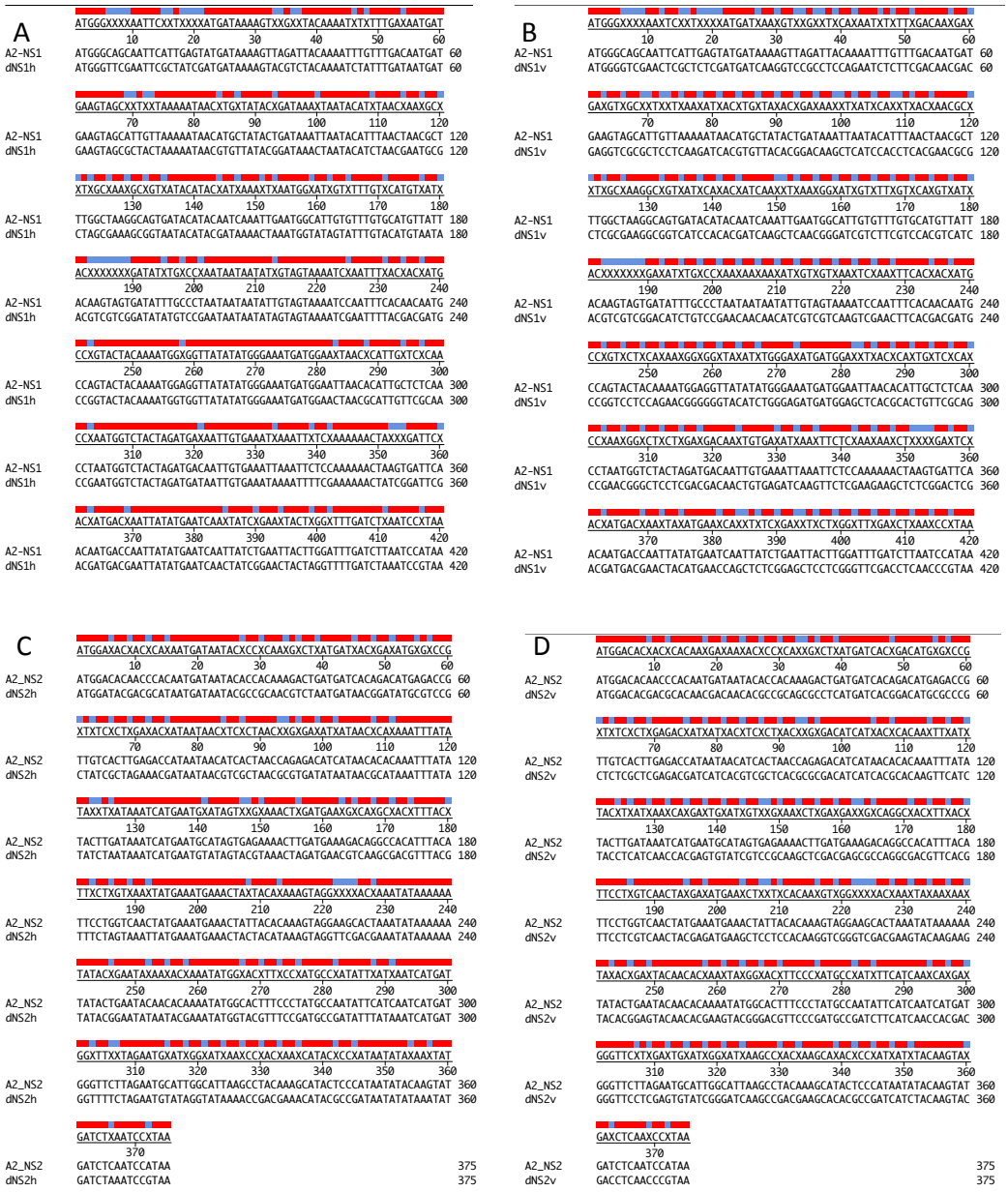

Fig 1. Nucleotide sequence alignment of RSV A2 strain NS1 and NS2 with human codon deoptimized NS1 and NS2.

(A and B) Nucleotide sequence alignment of RSV A2 strain NS1 open reading frame (ORF) with human codon deoptimized NS1 (dNS1h) (A) or virus codon deoptimized NS1 (dNS1v) (B) ORF. (C and D) Nucleotide sequence alignment of RSV A2 strain NS2 ORF with human codon deoptimized NS2 (dNS2h) (C) or virus codon deoptimized NS2

(dNS2v) (D) ORF. Nucleotide changes compared to A2 are highlighted in blue in the consensus sequences.

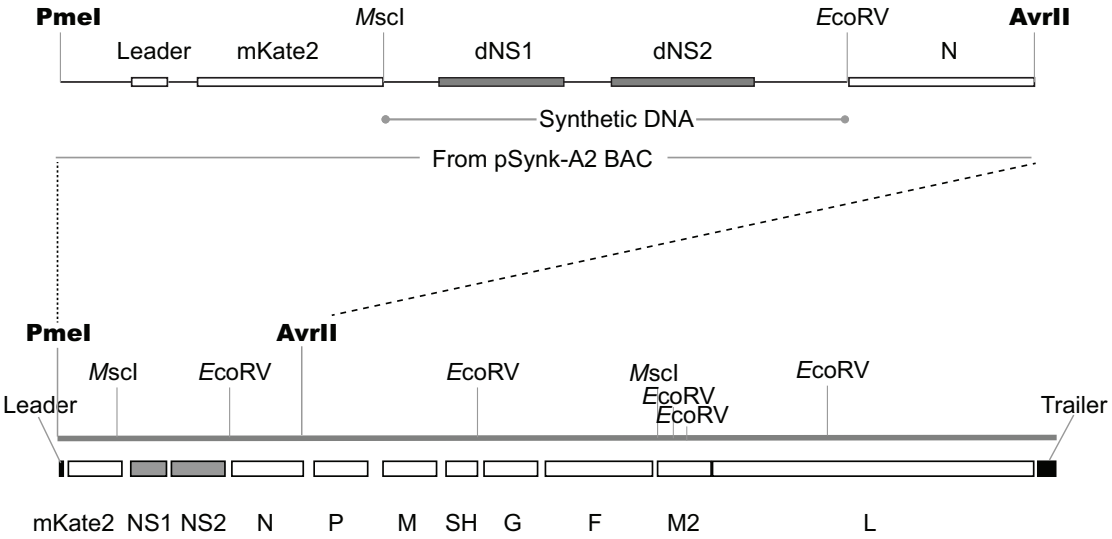

Fig 2. Generation of recombinant RSV with codon deoptimized NS1 and NS2. The PmeI-to-AvrII fragment from the parental RSV pSynk-A2 BAC clone was subcloned to replace the NS1 and NS2 regions with synthetic DNA containing the codon deoptimized NS1 and NS2 using MscI and EcoRV sites.

Reduced NS1 and NS2 protein expression by kRSV-dNSh *in vitro*

In order to examine the effect of codon deoptimization on NS1 and NS2 expression, HEp-2, BEAS-2B, and Vero cells were infected at a multiplicity of infection (MOI) of 5 with either parental kRSV-A2 or deoptimized virus kRSV-dNSh or kRSV-dNSv. Twenty-four hours postinfection (p.i.), total cell lysates were harvested and analyzed by Western blotting (Fig. 3). Relative steady-state NS1 and NS2 levels were determined by densitometry. Compared to kRSV-A2, human codon bias deoptimized virus (kRSV-dNSh) expressed 75 to 90% less NS1 protein and 70 to 90% less NS2 protein in these cell lines (Fig. 3). In contrast, RSV codon bias deoptimized virus (kRSV-

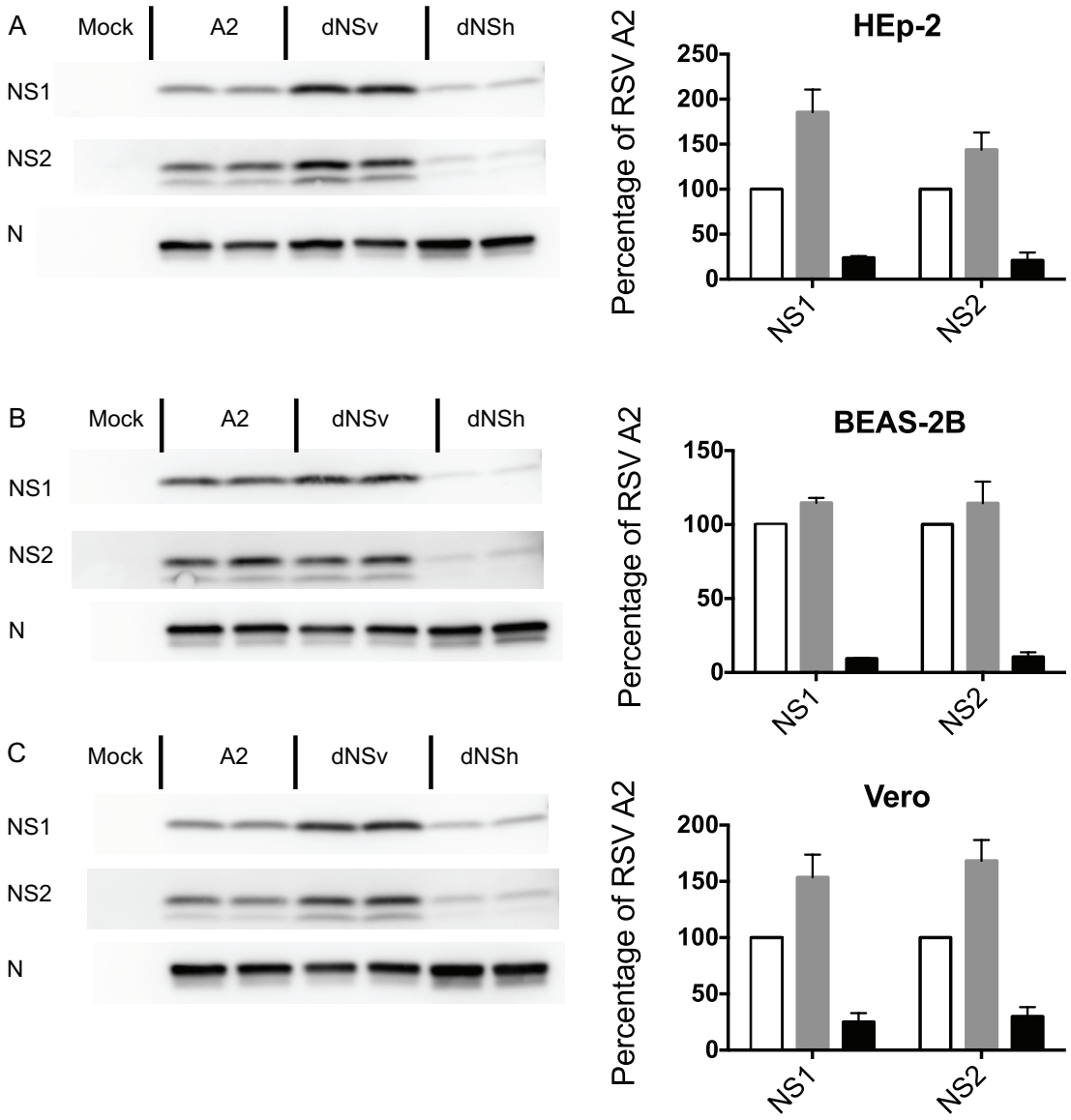

dNSv) expressed higher levels of NS1 and NS2 than did the parental virus, especially in HEp-2 and Vero cell lines (Fig. 3A and C). As the kRSV-dNSh virus exhibited the desired phenotype of reduced NS1 and NS2 levels, we chose this mutant for further studies.

Fig 3. Expression of NS1 and NS2 proteins during RSV infection in cell lines. HEp-2 (A), BEAS-2B (B), and Vero (C) cells were mock infected or infected with either kRSV-A2, kRSV-dNSv, or kRSV-dNSh at an MOI of 5. Twenty hours p.i., NS1 and NS2

protein levels were analyzed by Western blotting and densitometry. Representative blots are shown on the left. Densitometry results from 2 to 3 independent experiments are shown on the right. After normalization to RSV N protein expression level, NS1 and NS2 protein levels from each virus were normalized to those during kRSV-A2 infection and expressed as percentage ± SD. Unfilled bars represent kRSV-A2, gray bars represent kRSV-dNSv, and black bars represent kRSV-dNSh.

In vitro replication of human deoptimized NS1/NS2 RSV

Multistep growth curve analyses were done in several cell lines as well as primary, normal human bronchial epithelial (NHBE) cells differentiated at the air-liquid interface (ALI). kRSV-dNSh grew to similar levels as kRSV-A2 in HEp-2 and Vero cell lines (Fig. 4A and B). In BEAS-2B cells, the two viruses replicated to similar levels at earlier time points p.i., but growth of kRSV-dNSh was attenuated at 72 and 96 h p.i. (Fig. 4C). Primary differentiated airway epithelial cells provide a more accurate model than immortalized continuous cell lines for rank ordering RSV attenuation levels [63]. We therefore compared the growth kinetics of kRSV-dNSh and kRSV-A2 in differentiated NHBE/ALI cultures. At MOIs of 0.2 and 2.0, kRSV-dNSh virus exhibited a more restricted growth phenotype in these cell cultures, unlike kRSV-A2, which maintained its replication throughout the experiments (Fig. 4D to F). Although the two viruses started with similar levels of infection (Fig. 4F, day 1), only kRSV-A2 infectious yield increased (Fig. 4F). Similarly to previously published data, the RSV-infected NHBE cells exhibited no obvious cytopathic effect over the course of infection (Fig. 4F) [60].

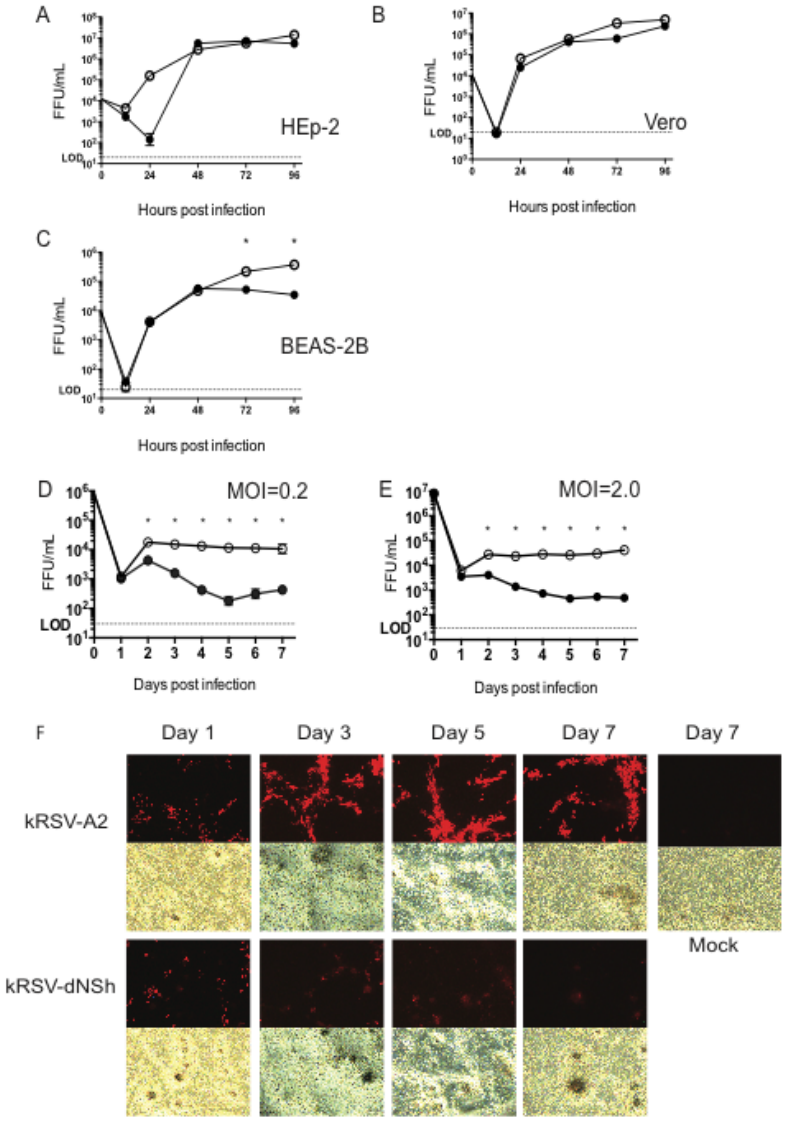

Fig 4. Growth kinetics of kRSV-A2 and kRSV-dNSh *in vitro*.

(A to E) Growth kinetics of kRSV-A2 (open circles) and kRSV-dNSh (closed circles) in HEp-2 (A), Vero (B), and BEAS-2B (C) cells at 37 °C infected at an MOI of 0.01, as well as in differentiated NHBE/ALI cells infected at an MOI of 0.2 (D) and 2.0 (E). (F) Time course images for NHBE cells infected at an MOI of 0.2, showing mKate2 fluorescence produced by recombinant viruses. For growth curves in panels A, B, and C, each graph is compiled from two independent experiments performed in duplicate wells.

For panels D and E, each single experiment was performed in triplicate wells. *, $P < 0.05$ between kRSV-dNSh- and kRSV-A2-infected groups. NHBE, normal human bronchial epithelial cells; ALI, air-liquid interface; LOD, limit of detection.

Attenuation, protection, and immunogenicity in BALB/c mice

BALB/c mice were infected with either kRSV-A2 or kRSV-dNSh virus, and lung viral loads were measured at indicated days postinfection. Both viruses peaked between days 4 and 6, and kRSV-dNSh exhibited approximately a 1-$\log_{10}$-lower titer than kRSV-A2 on both days (Fig. 5A). As complete protection against RSV challenge is commonly achieved in the BALB/c mouse model with experimental RSV vaccines, we increased the stringency of efficacy determination in this model by using a dose titration of vaccines to evaluate breakthrough of protection. When given as a single vaccination of 10^5 fluorescent focus units (FFU) intranasally (i.n.), both kRSV-A2 and kRSV-dNSh elicited complete protection against heterologous subgroup A RSV strain A/1997/12-35 (12-35 [73]) challenge at 100 days postvaccination (Fig. 5B). Vaccination using kRSV-A2 or kRSV-dNSh with 10^4 or 10^3 FFU resulted in equivalent levels of protection and breakthrough. This protection correlated with induction of RSV-neutralizing antibodies (nAb) over time, and kRSV-dNSh induced slightly but statistically significantly higher levels of nAb than did kRSV-A2 (Fig. 5C). Mice vaccinated with a dose range of either kRSV-A2 or kRSV-dNSh also showed similar levels of protection against challenge with RSV A2-line19F at day 28 postvaccination (Fig. 5D). Taken together, kRSV-dNSh was significantly attenuated in mice but was equally protective and slightly more immunogenic than the parental kRSV-A2 strain.

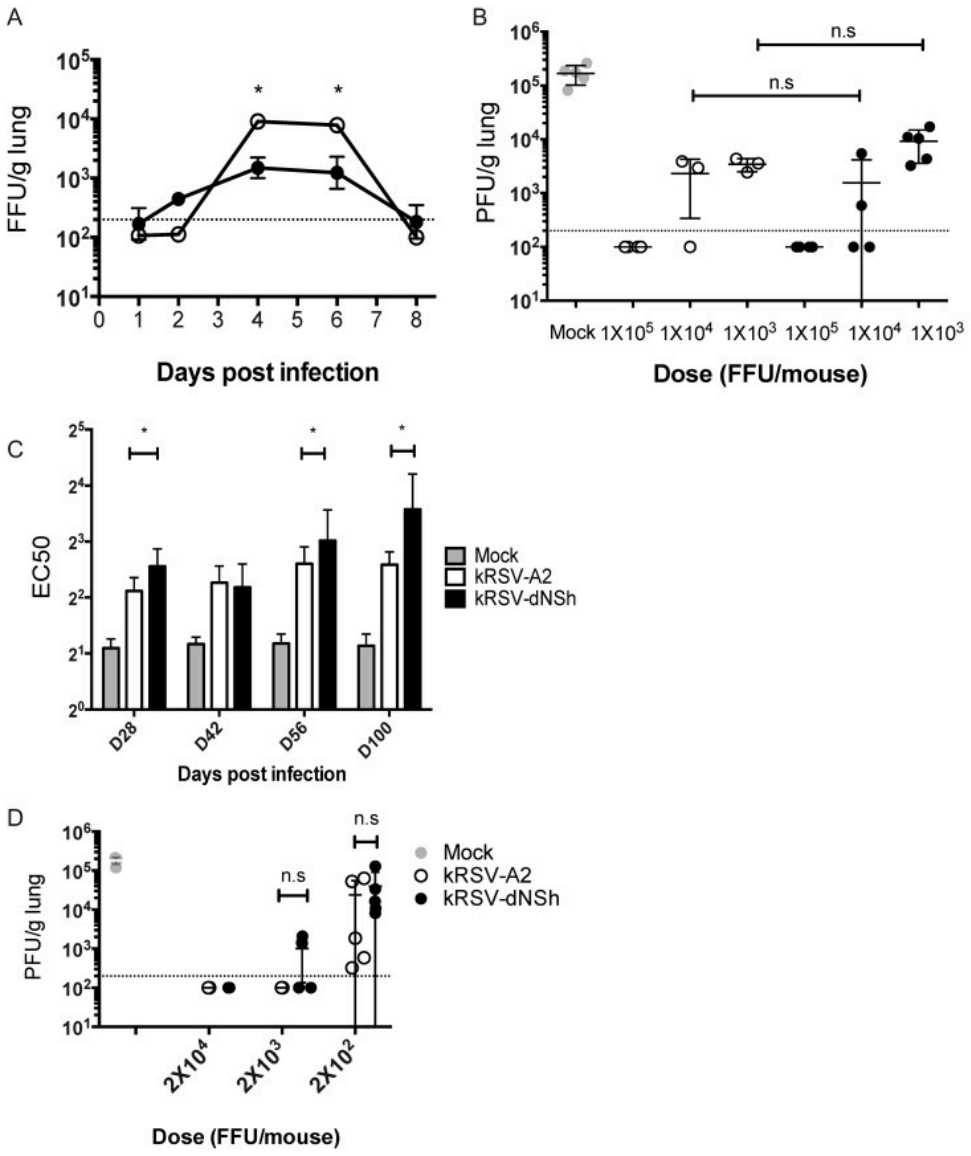

Fig 5. Attenuation, efficacy, and immunogenicity.

(A) BALB/c mice (5 per group) were infected i.n. with either kRSV-A2 (open circles) or kRSV-dNSh (closed circles), and lung viral loads on indicated days are shown. *, $P <$ 0.05 comparing kRSV-A2 to kRSV-dNSh at days 4 and 6. (B) BALB/c mice (5 per group) were vaccinated i.n. with various doses of either kRSV-A2 (open circles) or kRSV-dNSh (closed circles) or mock infected (grey circles) and challenged with the RSV 12-35 strain 100 days later. Lung peak viral loads after challenge are shown. Each

symbol represents a single mouse. (C) Serum nAb titers measured at indicated days after vaccination with 1×10^5 FFU. There were 5 mice per group. *, $P < 0.05$ comparing the bracketed kRSV-dNSh- and kRSV-A2-infected groups. (D) Lung peak viral loads after rA2-line19F challenge 28 days postvaccination. Each symbol represents a single mouse. All data represent one of two replicate experiments with similar results. Dotted lines indicate limit of detection for plaque assay. i.n., intranasal; FFU, fluorescent focus unit; PFU, plaque-forming unit; n.s., not significant.

STAT2 degradation and NF-κB activation

We characterized the effect of kRSV-dNSh infection on STAT2, a known target for NS2 and potentially NS1 [84, 85, 88, 89, 92]. 293T cells were mock infected or infected with either wild-type kRSV-A2 or kRSV-dNSh. As expected, kRSV-A2 infection caused 50% STAT2 degradation compared to mock infection. In contrast, we found that kRSV-dNSh infection had no effect on STAT2 levels compared to mock infection (Fig. 6A), suggesting that reduced NS1 and NS2 protein levels may augment host immune responses due to less STAT2 degradation compared to wild-type virus infection.

Early during RSV infection, NS1 and NS2 proteins activate host cell prosurvival signals to promote viral growth, including NF-κB, so that NF-κB activation is a measure of NS1/NS2 function [91, 94]. Activation of NF-κB leads to expression of proinflammatory cytokines. Pediatric live-attenuated vaccine strains should preferably be less proinflammatory than wild-type strains for safety concerns. HEK-Blue-Null 1 cells,

which contain an NF-κB reporter gene, were mock infected or infected with kRSV-A2 or kRSV-dNSh. Tumor necrosis factor alpha (TNF-α), as a positive control for NF-κB activation, induced a high level of reporter activity, followed by kRSV-A2 virus infection (Fig. 6B). Mock infection and kRSV-dNSh infection resulted in equivalent low levels of NF-κB activation, indicating a reduced NF-κB activation and inflammatory potential of kRSV-dNSh compared to the wild-type virus.

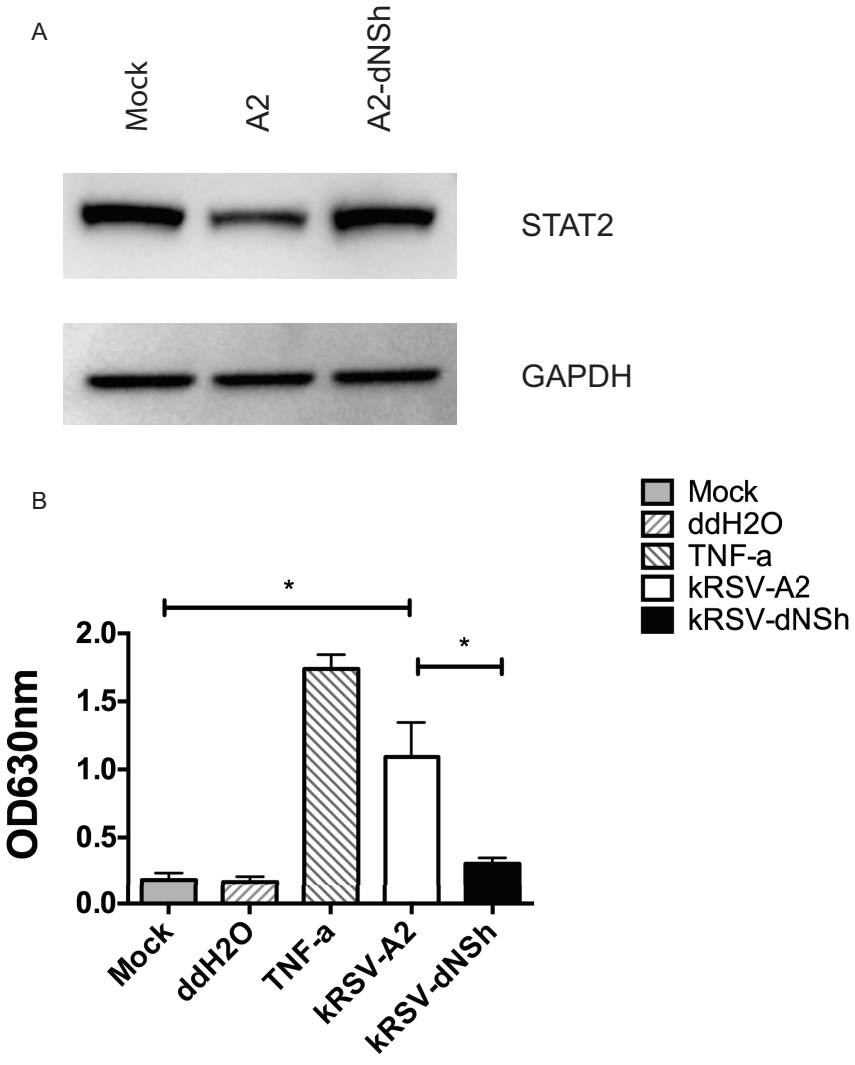

Fig 6. STAT2 degradation and NF-κB activation.

(A) 293T cells infected with either kRSV-A2 or kRSV-dNSh or mock infected at an MOI of 3. Twenty hours p.i., total STAT2 protein level was analyzed by Western blotting and

densitometry (from three independent experiments). (B) HEK-Blue-Null 1 cells treated with either kRSV-A2, kRSV-dNSh, mock treatment, TNF-α (1ng/mL), or double-distilled water (ddH_2O) for 72 h. Supernatants were measured for reporter activity using a colorimetric assay (from three independent experiments). *, $P < 0.05$ between the groups indicated by the open brackets.

DISCUSSION

Here, we adapted the codon deoptimization strategy to specifically target RSV nonessential virulence genes NS1 and NS2, which function in immune suppression. Deoptimization was based on human codon usage bias, which resulted in reduced target protein expression. Unlike previous RSV attenuation strategies focusing on virus replication *per se*, diminishing expression of NS1 and NS2 led to attenuation without loss of immunogenicity or infectious yield in Vero cells. Codon deoptimization of nonessential target virulence genes can simultaneously fine-tune attenuation and immunogenicity. The stability of the recoded sequences was also confirmed by *in vitro* passaging the virus stocks in a restrictive cell line (BEAS-2B) without new mutations.

NS1 and NS2 proteins of RSV suppress type I and type III IFN responses in human epithelial cells [90, 92, 100]. Homologous genes in related viruses, pneumonia virus of mice (PVM) and bovine respiratory syncytial virus (BRSV), also antagonize type I and type III IFN responses [128-131]. Targets of NS1 and NS2 genes include various members of the type I IFN pathways, including STAT2 [84-89, 92]. In agreement with these studies, we found that STAT2 protein levels were reduced in kRSV-A2 infection but not during kRSV-dNSh infection. There is functional overlap between NS1 and NS2 proteins [84, 88, 90, 91, 100, 102]. For example, NS1 and NS2 can cooperatively suppress the maturation of dendritic cells (DC), as ΔNS1/NS2 RSV treatment resulted in higher DC maturation than did ΔNS1 or ΔNS2 treatment [102]. Both NS1 and NS2 inhibit IRF3 activation in human epithelial cells [91]. Both genes inhibit induction of human alpha interferon (IFN-α), IFN-β, and IFN-λ [90]. The overlapping functions of

NS1 and NS2 could be explained by their potential interaction and formation of multi-subunit complexes in the infected cell [85, 92, 132]. Collectively, these studies show that double deletion of NS1 and NS2 attenuates the virus more than the single deletions and induces the highest level of antiviral immune responses, supporting our strategy to target both nonstructural genes of RSV.

Deletion of either RSV NS gene or both results in virus attenuation both *in vitro* and *in vivo* [90, 95-98, 133]. ΔNS1 and ΔNS2 single deletion mutants and the ΔNS1/NS2 double deletion mutant replicate at lower levels than wild-type virus, with ΔNS2 only slightly attenuated and ΔNS1/NS2 about 2 $\log_{10}$ attenuated in BALB/c mice [100]. We found that kRSV-dNSh virus had a milder phenotype than ΔNS1/NS2 because kRSV-dNSh was 1 $\log_{10}$ attenuated as a vaccine. Also, kRSV-dNSh virus was not attenuated in Vero cells, the presumed vaccine strain producer cells, unlike ΔNS1/NS2, which exhibited a 20-fold-lower titer in Vero cells [90].

Transcription factor NF-κB activates many host antiapoptotic and proinflammatory genes and is activated by NS1 and NS2 genes rapidly during RSV infection to delay apoptosis [91, 94]. Blocking apoptosis by activation of NF-κB to promote viral replication has been documented for other viruses, such as HIV-1, influenza virus, hepatitis B virus (HBV), and HCV [134]. We speculate that reduced NF-κB activation by kRSV-dNSh, compared to kRSV-A2, may contribute to the attenuated phenotype of this mutant due to accelerated cell death (Fig. 6B).

Virus attenuation through manipulation of codon usage or codon pair usage in conjunction with synthetic biology has been achieved for several viruses, including poliovirus and influenza virus [124-126, 135, 136]. Rather than recoding the protein sequence by using the rarest codons for each amino acid (codon deoptimization), codon pair deoptimization recodes the protein sequence to maximize the occurrence of the rarest adjacent codon pairs. The mechanisms behind virus attenuation using either method are not completely defined. Decreased translational efficiency of codon deoptimized or codon-pair deoptimized genes is considered the main principle, although mRNA stability was not examined in each case [125, 126, 135, 136]. According to the "mutation-selection-drift balance" model, codon bias may be under weak selection for translation efficiency or accuracy, although other mechanisms are proposed, such as mutational bias [137]. Studies of tRNA concentration either by gene copy number or by direct measure of cellular tRNA pools have provided a consistent correlation between tRNA abundance and corresponding codon usage frequency, lending support to translational selection on codon bias [138]. Codon usage appears to be an important cellular strategy to control protein expression level, activity, function, and ultimately physiology [139-142]. Other than selection on translation efficiency, codon usage pattern has also been implicated in regulating the protein-folding process [142, 143]. Thus, the production of a functional protein from mRNA is tightly regulated by its codon usage pattern in every step of the process.

We propose codon deoptimization of nonessential virus virulence genes as a general strategy in generating live-attenuated vaccine candidates with retained

immunogenicity *in vivo*, genetic stability, and replication in producer cell lines *in vitro*. This may be important for RSV vaccines because the wild-type virus is not potently immunogenic and does not grow to high titers *in vitro*. Additionally, reversion to wild-type virulence in the context of codon deoptimization is minimized due to the additive contribution of silent mutations across the coding region [126], and out *in vitro* serial passaging experiment provided support for this. Because the recoding method does not change protein sequence, it will maximally preserve immune epitopes. Although more studies are needed to understand the effect of recoding protein sequences using either rare codons or codon pairs on protein translation, targeting virulence genes using this method should be widely applicable to many viruses for live-attenuated vaccine development.

MATERIALS AND METHODS

Cell lines. Vero (ATCC CCL-81) and HEp-2 (ATCC CCL-23) cells were maintained in minimal essential medium (MEM) with Earle's salts and L-glutamine (Gibco) supplemented with 10% fetal bovine serum (FBS) (HyClone) and 1 μg/mL penicillin, streptomycin sulfate, and amphotericin B solution (PSA) (Invitrogen). BEAS-2B cells were maintained in RPMI 1640 (Cellgro) with 10% FBS, as described previously [73]. HEK-Blue Null 1 cells, which express secreted embryonic alkaline phosphatase (SEAP) under the control of the IFN-β minimal promoter fused to NF-κB and AP-1 binding sites, were maintained in Dulbecco's modified Eagle medium supplemented with 10% FBS, L-glutamine, 4.5 g/liter D-glucose, and 1 μg/mL PSA, as recommended by the provider (InvivoGen, San Diego, CA). BSR-T7/5 cells were a gift from Ursula Buchholz (National Institute of Health, Bethesda, MS) and were cultured in Glasgow's minimal essential medium (GMEM) containing 10% FBS and 1 μg/mL PSA. BSR-T7/5 cells were selected with 1mg/mL Geneticin every other passage.

RSV strains. We performed RSV reverse genetics by cotransfection of five plasmids, an RSV antigenomic cDNA cloned in a bacterial artificial chromosome (BAC) and four codon-optimized helper plasmids that express RSV N, P, M2-1, or L protein, into BSR-T7/5 cells as we described previously [53]. The pSynkRSV-line19F BAC produces A2-line19F RSV with the far-red fluorescent protein monomeric Katushka-2 (mKate2) in the first position [53] to mark infected cells. We modified pSynkRSV-line19F by replacing the line 19 strain fusion (F) gene, flanked by SacII-to-SalI sites in the BAC, with a synthetic cDNA (GeneArt) containing the A2strain F open reading

frame (A2 from Barney Graham, Vanderbilt University; GenBank accession number FJ614814) flanked by noncoding regions identical to those in pSynkRSV-line19F and corresponding SacII-to-SalI sites [53]. The resulting BAC (pSynk-A2) was used as the genetic background for insertion of codon deoptimized RSV nonstructural (NS) genes. The PmeI-AvrII fragment from pSynk-A2 BAC (Fig. 2) was subcloned. The MscI-to-EcoRV fragment of pSynk-A2 was replaced with a corresponding synthetic fragment (GeneArt, Life Technologies, Gaithersburg, MD) in which only the NS1 and NS2 open reading frames were codon deoptimized based on either human or viral codon usage to generate kRSV-dNSh or kRSV-dNSv, respectively. Recombinant RSV was recovered by transfection as described previously, except that virus stocks were propagated in Vero cells [53]. All the virus stocks used in this study were sequenced for the NS1 and NS2 genes and confirmed to be mycoplasma negative using the Venor GeM *Mycoplasma* detection kit (Sigma-Aldrich, At. Louis, MO). Challenge virus strains A2-line19F and RSV 12-35 were generated in HEp-2 cells as described previously and tittered by plaque assay on HEp-2 cells [73].

Normal human bronchial epithelial cells at air-liquid interface (NHBE/ALI). NHBE cells (Lonza, Allendale, NJ) were cultured according to the recommended protocols. Cells were seeded onto collagen-coated (BD Biosciences, Bedford, MA) 24-well transwell supports (Corning Costar, NY) for differentiation. Briefly, 5×10^4 cells (100 μL) in B-ALI growth medium (Lonza) were seeded per insert with 500 μL B-ALI growth medium added to the basal chamber. Growth medium in both apical and basal chambers was changed the next day. Air-lift was performed on day 3 by removing B-ALI

growth medium from both chambers followed by adding 500 μL b-ALI differentiation medium (Lonza) supplemented with inducer only to the basal chamber. Differentiation medium in the basal chamber was replaced with fresh medium every other day for 21 days before experiments.

Western blotting. Cells (HEp-2, Vero, or BEAS-2B) at 70% confluence were infected with kRSV-A2, kRSV-dNSh, or kRSV-dNSv at an MOI of 5, and cell lysates were harvested 20 h p.i. in RIPA buffer (Sigma-Aldrich, St. Louis, MO) containing 1 × protease inhibitor cocktail (Thermo Scientific, Rockford, IL). Proteins were separated by SDS-PAGE and transferred onto polyvinylidene difluoride membranes. Blots were blocked with 5% nonfat milk in Tris-buffered (TBS) plus 0.1% Tween 20. Polyclonal rabbit antisera against NS1 and NS2 proteins (gifts from Michael Teng, USF Health) were used to quantify protein levels. Blots were stripped and reprobed with a mouse monoclonal antibody against RSV N protein (clone D14, a gift from Edward Walsh) as a loading control. For STAT2 protein detection, 293T cells at 70% confluence were mock infected or infected with either kRSV-A2 or kRSV-dNSh virus at an MOI of 3. Cell lysates were harvested 12 h later. Blots were probed with rabbit anti-STAT2 polyclonal antibody (C2; Santa Cruz Biotechnology, Santa Cruz, CA). Blots were stripped and reprobed with mouse anti-glyceraldehyde-3-phosphate dehydrogenase (anti-GAPDH) antibody (6C5; GeneTex, Irvine, CA) as a loading control.

FFU assay. Vero cells at 70% confluence in 96-well plates were inoculated with 50 μL of 10-fold serial dilutions of samples. Inoculation was carried out at room

temperature with gentle rocking for 1 h before 0.75% methylcellulose (EMD, Gibbstown, NJ) dissolved in MEM supplemented with 10% FBS and 1% PSA was added. Cells were incubated for 48 h before counting FFU per well. The limit of detection is 1 FFU per well, corresponding to 20 FFU/mL.

Virus growth kinetics. Seventy percent confluent cells in 6-well plates were infected at an MOI of 0.01 in a volume of 500 μL. After 1-h incubation at room temperature, cells were washed once with 2 mL of phosphate-buffered saline (PBS), and 2 mL MEM with 10% FBS (for the Vero cell line) or RPMI 1640 with 10% FBS (for the BEAS-2B cell line) was added. At time points p.i., cells were scraped in medium and resuspended, and aliquots were frozen until use. Differentiated NHBE cells were infected at an MOI of 0.2 or 2. Virus inoculum (100 μL) was applied apically after PBS wash (100 μL) followed by a 2-h incubation at 37 °C. Inoculum was removed by three apical PBS washes. To collect virus for time points, differentiated medium without inducer (150 μL) was added to the apical chamber and cells were incubated for 10 min at 37 °C. This step was repeated twice for each well (300 μL total). This apical supernatant was snap-frozen in liquid nitrogen and stored until use.

Viral load and protection and vaccine efficacy. All animal studies were approved by the Emory University Institutional Animal Care and Use Committee (protocol number 2001533) and carried out in accordance with recommendations in the Guide for Care and Use of Laboratory Animals of the National Institutes of Health, as well as local, state, and federal laws. Six- to eight-week-old female BALB/c mice (The

Jackson Laboratory, Bar Harbor, ME) maintained under specific-pathogen-free conditions were intranasally (i.n.) infected with 1.6×10^5 FFU of virus per mouse. The left lung from each mouse was harvested for viral titer by FFU assay (described above) at days 1, 2, 4, 6, and 8 postinfection. For vaccine protection and efficacy assays, mice were vaccinated with various does of either kRSV-A2 or kRSV-dNSh i.n. and challenged with either 1.6×10^6 PFU of RSV 12-35 [73] at 100 days after vaccination or 2×10^6 PFU of A2-line19F at 28 days after vaccination. For mice infected with 1×10^5 FFU vaccine virus and challenged 100 days postinfection, serum samples were collected on days 28, 42, 56, and 100 by mandibular bleeding. Lung peak viral loads postchallenge were measured on day 4 after challenge by plaque assay as described in reference [73]. For all mouse experiments, n was 5 per group. Titers below the limit of detection were assigned half the value of the limit of detection.

Microneutralization assay. HEp-2 cells were seeded in 96-well plates to attain 70% confluence in 24 h. Heat-inactivated (56 °C, 30min) serum samples were 2-fold serially diluted in MEM and added to 50 to 100 FFU kRSV-A2 in an equal volume. The virus and serum mixture was incubated at 37 °C for 1 h. Then, half of the serum-virus mixture was transferred onto HEp-2 cell monolayers in 96-well plates in duplicate, and plates were spinoculated at 2,000 × g for 30 min at 4 °C. Fluorescent foci were counted 36 h p.i.. The 50% effective concentration (EC_{50}) was calculated using a nonlinear regression analysis with four-parameter fitting in GraphPad Prism version 6.0.

NF-κB activation assay. NF-κB activity was assayed according to the manufacturer's protocol (InvivoGen, San Diego, CA). Briefly, HEK-Blue-Null 1 cells were seeded at 5×10^4/well in a 96-well plate and infected with either kRSV-A2 or kRSV-dNSh or mock infected for 72 h. Supernatants were incubated with Quanti-Blue (InvivoGen, San Diego, CA) substrate prepared according to instructions for 1 to 3 h before reading optical density at 630 nm on a microplate reader (Bio-Tek, Winooski, VT).

Statistical analysis. Statistical analysis was performed using GraphPad Prism software version 6.0 (San Diego, CA). Data are represented as means with standard deviation (SDs). One-way and two-way analyses of variance (ANOVA) with Tukey's *post hoc* test with a *P* value of 0.05 were used, as indicated. Student's *t* test (unpaired, two-tailed) was used for Fig. 6A.

ACKNOWLEDGMENTS

This work was supported by NIH grants 1R01AI087798 and 1U19AI095227 and by Emory University and Children's Healthcare of Atlanta funds.

We thank Edward Walsh for monoclonal antibody to RSV N protein and Michael Teng for antisera to RSV NS1 and NS2 proteins. We thank Ursula Buchholz and Karl-Klaus Conzelmann for BSR-T7/5 cells.

M.L.M. and Emory University are entitled to licensing fees derived from various agreements Emory has entered into related to products used in the research described in

this paper. This study could affect his personal financial status. The terms of this agreement have been reviewed and approved by Emory University in accordance with its conflict of interest policies.

CHAPTER 3

The Contribution of Attachment Glycoprotein to Respiratory Syncytial Virus Infection Depends on the Specific Fusion Protein

This part of the thesis is in preparation for submission to Journal of Virology as of April 2015

The Contribution of Attachment Glycoprotein to Respiratory Syncytial Virus Infection Depends on the Specific Fusion Protein

Jia Meng[a, b], Michael G. Currier[a, b], Sujin Lee[a, b], Martin L. Moore[a, b]

[a]Department of Pediatrics, Emory University School of Medicine, Atlanta, Georgia, USA

[b]Children's Healthcare of Atlanta, Atlanta, Georgia, USA

Address correspondence to Martin L. Moore, martin.moore@emory.edu

ABSTRACT

Human respiratory syncytial virus (RSV) is an important pathogen causing acute lower respiratory tract disease in children. The RSV attachment glycoprotein (G) is not required for infection, as G-null RSV replicates efficiently in several cell lines. Our laboratory previously reported that the viral fusion (F) protein is a determinant of strain-dependent pathogenesis. Here, we hypothesized that virus dependence on G is determined by the strain specificity of F. To test our hypothesis, we generated recombinant viruses expressing G and F, or null for G, from the laboratory A2 strain (kRSV-A2G-A2F and kRSV-GstopA2F) or the clinical isolate A2001/2-20 (kRSV-2-20G-2-20F and kRSV-Gstop2-20F). We quantified virus cell binding, entry kinetics, infectivity, and growth kinetics *in vitro*. 2-20 G expressing virus exhibited the greatest binding activity. Compared to the parental viruses expressing G and F, removal of 2-20 G had more deleterious effects on binding, entry, infectivity, and growth than removal of A2 G. Overall, RSV expressing 2-20 F had a high dependence on G for binding and infection.

INTRODUCTION

Human respiratory syncytial virus (RSV) causes an annual global 3.4 million estimated severe acute lower respiratory infections (ALRI) in children younger than 5 years of age, necessitating hospitalization and medical interventions [1]. In the US, about 132,000 to 172,000 children younger than 5 years old are hospitalized due to RSV every year [2]. Not only does RSV infect and cause severe disease in the very young population, it also causes great burden in elderly adults [144, 145]. Despite several decades of research efforts on generating a safe and efficacious vaccine for this virus, so far, there is no licensed vaccine. There are multiple vaccine platforms currently undergoing early phases of clinical trials [107], and development of more effective antivirals against RSV is also an active field of research [146-148].

RSV is a member of the *Paramyxoviridae* family, *Pneumovirus* genus. The *Paramyxoviridae* family also includes other important human and animal pathogens such as measles virus, parainfluenza viruses, human metapneumovirus, Sendai virus, canine distemper virus, and the more recently identified Nipah and Hendra viruses. Members of the *Paramyxoviridae* family encode two major glycoproteins involved in the early infection process, attachment to the host cell and subsequent entry process. The paramyxovirus fusion process generally involves F triggering by the homologous attachment protein upon receptor engagement (reviewed in [149, 150]). However, previous studies with RSV glycoproteins (F and G) indicate that this is not a strict requirement for RSV fusion protein [149-151]. The attachment protein G has long been thought to mediate the majority of virus binding to host cell glycosaminoglycans (GAGs)

[34, 59, 152] with limited contributions to triggering the fusion process. However, this attachment function can be substituted by the F protein [153]. Several studies on both subgroup A and B RSV strains indicate that G is not functionally required for efficient *in vitro* replication in certain cell lines, but is needed for optimal growth *in vivo* [11, 35, 59]. This is in sharp contrast to the other paramyxoviruses, of which the fusion protein requires the homologous attachment protein to function optimally.

Considering that all the previous studies regarding the requirement for G function during RSV infection were done with lab-adapted strains of this virus, we set out to re-evaluate the functions of this major attachment protein from a clinical isolate strain and compared these functions with the lab-adapted strain A2. We generated recombinant RSV strains harboring different combinations of the F and G proteins (GF virus, kRSV-A2G-A2F and kRSV-2-20G-2-20F), along with viruses that do not express the G gene but maintain almost identical genomic sequence composition in the G gene region (Gstop virus, kRSV-GstopA2F and kRSV-Gstop2-20F), in order to maintain the overall transcriptional integrity of all the recombinant viruses. By comparing the G functions between each GF virus and Gstop virus pair, we found that there are certain functions of the attachment protein unique to the clinical strain, but not the A2 lab-adapted strain. These functions include enhanced binding to the cell, enhancement of F-mediated cell-to-cell fusion, viral entry, infectivity, and overall *in vitro* growth rate. Our study has suggests some interesting properties of the G attachment protein, especially relating to the fusion process, that have been over-looked by using lab-adapted strains. The

generality of the current study could be further addressed by using additional RSV clinical isolates.

MATERIALS AND METHODS

Cell lines. HEp-2 (ATCC CCL-23) and 293T (ATCC, CRL-3216) cells were maintained in minimal essential medium (MEM) with Earle's salts and L-glutamine (Gibco) supplemented with 10% fetal bovine serum (FBS) (HyClone) and 1 μg/mL penicillin, streptomycin sulfate, and amphotericin B solution (PSA) (Invitrogen). BEAS-2B cells were maintained in RPMI 1640 (Cellgro) with 10% FBS and 1 μg/mL PSA as described [73]. BSR-T7/5 cells (a gift from Dr. Ursula Buchholz, National Institute of Health, Bethesda, MD) were cultured in Glasgow's minimal essential medium (GMEM) containing 10% FBS and 1 μg/mL PSA, and every other passage these cells were selected with geneticin at 1mg/mL. Chinese hamster ovary (CHO-K1) (ATCC, CCL-61) cells and a heparin sulfate-deficient derivative of this cell line, pgsD-677 (ATCC, CRL-2244) cells were cultured in Kaighn's modified F-12K (+L-glutamine) (Gibco) supplemented with 10% FBS and 1 μg/mL PSA, according to ATCC instructions.

Generation of recombinant RSV strains. The G and F glycoprotein genes (RSV G GenBank accession number JF279545 and RSV F GenBank accession number JF279544) of RSV A2001/2-20 [73] were synthesized by GeneArt (Life Technologies, Grand Island, NY) and cloned into a bacterial artificial chromosome (BAC) containing the antigenomic cDNA of RSV A2, described previously [53]. All recombinant RSV strains generated in this study express a far-red fluorescent gene (monomeric Katushka-2, mKate2) in the first gene position. To generate the recombinant RSV strains without G protein expression (Gstop viruses), both of the *Met codons* (Met_1 and Met_{48}) in the G open reading frame (ORF) were changed to *Ile* with the first *Met*/*Ile* followed by a stop codon

[35]. Recombinant viruses were recovered by co-transfection of the RSV antigenomic BAC and four human codon bias-optimized RSV helper plasmids (N, P, L, and M2-1) into BSR-T7/5 cells as described previously [53]. The viruses were propagated in HEp-2 cells and sequence confirmed for the glycoprotein ORFs. Viruses used in this study were prepared by harvesting infected HEp-2 cells followed by sonication, as described [154]. For binding assays, the virus stocks were purified by sucrose gradient centrifugation to remove the majority of the cellular proteins from the virus fraction [155]. Briefly, the infected HEp-2 cells were frozen in -80 °C and later thawed at 37 °C. Cells were scraped and along with the medium were transferred to 50 mL conical tubes. After centrifugation at 2000 rpm for 10 min at 4 °C, supernatants were pooled and layered onto 20% sucrose-containing MEM for subsequent ultracentrifugation at 16,000 × g for 3 hours at 4 °C (SW32 rotor, Beckman Coulter). The resulting pellets were resuspended in MEM and aliquots were frozen in liquid nitrogen before storing in -80 °C until use.

RSV binding assay and Western blotting. BEAS-2B cells were seeded the day before to be subconfluent for the experiment. Input volumes of sucrose purified virus stocks were determined by Western blotting of RSV N protein levels. The cells were washed with cold PBS, placed on ice, and inoculated with virus for 2 hours. Then the inoculums were removed by three ice-cold PBS wash, and cells were lysed in RIPA buffer (Sigma-Aldrich, St. Louis, MO) supplemented with 1 X protease inhibitors cocktail (Thermo Scientific, Rockford, IL). The lysates were cleared by centrifugation at 13.2K rpm for 10 min at 4 °C and supernatants were used for Western blotting. To compare the amount of virus bound in each sample, the intensity of RSV N protein band

was normalized to the glyceraldehyde-3-phosphate dehydrogenase (GAPDH) band of the same sample. This normalized intensity of RSV N protein was then used in the final analysis of bound virus.

Protein samples were mixed with 2 X Laemmli sample buffer (Sigma-Aldrich, St. Louis, MO) and heated at 95 °C for 10 min with shaking at 350 rpm. Samples were separated on a 10% SDS-PAGE gel and transferred onto polyvinylidene difluoride (PVDF) membranes and blocked with 5% non-fat milk in Tris-buffered saline (TBS) containing 0.1% Tween-20. Blots were probed with a mouse monoclonal antibody (clone D14, generously provided by Dr. Edward Walsh, University of Rochester, New York) against RSV N protein followed by a horseradish peroxidase conjugated secondary antibody. For GAPDH blots, mouse anti-GAPDH (6C5, GeneTex, Irvine, CA) was used. Chemiluminescent signals were detected with WesternBright Quantum substrates (Advansta, Menlo Park, CA) on a ChemiDoc imaging system (Bio-Rad, Hercules, CA).

Fluorescent focus unit (FFU) assay. HEp-2 cells were seeded in 96-well flat-bottom plates the day before to reach 70% confluence for the assay. Fifty microliters of 10-fold serial diluted virus samples were inoculated onto the cells and incubated 1.5 hr at room temperature with gentle rocking. After virus adsorption, 150 μL 0.75% methylcellulose (EMD, Gibbstown, NJ) in complete media was added to each well, then plates were incubated at 37 °C 5% CO_2 for 2 days. Wells containing 5-50 fluorescent focus units (FFU) were counted and used for the calculation of the virus titer in the

samples. The limit of detection of this assay is 1 FFU per well, corresponding to 20 FFU/mL.

Infectivity and virus growth kinetics. Cells were seeded into 6-well plates the day before to be 70% confluence for infection at 1.0 multiplicity of infection (MOI). Cells were washed with PBS once before infection in a total volume of 500 μL per well at room temperature for 1 hour with gentle rocking. The cells were then washed twice with PBS to remove any remaining inoculum. For infectivity, cells were trypsinized 20 hr post-infection and quantified using a flow cytometer LSRII (Becton Dickinson, NJ), detecting the mKate2 signal with a 532 nm laser with a 610/20 filter. For growth kinetics, triplicate wells of cells were scraped in medium and resuspended at the indicated times, and aliquots of samples frozen in -80 °C until titration by the FFU assay described above.

RSV entry assay. This assay was performed as described previously with some modifications [156]. BEAS-2B cells (70% confluent in 12-well plates) were placed on ice for 5 min, washed once with ice-cold PBS before addition of the virus at an MOI of 1.0. Binding of the virus to the cells proceeded for two hours on ice with gentle shaking until the inoculums were removed and cells washed twice with ice-cold PBS. Five hundred microliters of ice-cold RPMI 1640 medium was added to each well. Plates were then warmed up in 37 °C water bath for the indicated times (30 sec, 1, 2, 3, 4, and 5 min) one time point at a time. At the end of each time point, medium was removed followed by addition of 500 μL citrate buffer (400 mM sodium citrate, 10 mM potassium chloride, 135 mM sodium chloride, pH 3.0) for 2 minutes to inactivate any remaining extracellular

virus. Cells were then washed in room temperature PBS once before addition of medium and continuing incubation at 37 °C 5% CO_2 for 20 hours. Infected (mKate2+) cells were counted on an LSRII cytometer.

Dual-split protein (DSP) fusion assay. We previously used this assay to quantify cell-cell fusion activity of expressed RSV F proteins [157, 158]. 293T cells in 6-well plates were transfected with 500 fmol of reporter plasmids DSP_{1-7} or DSP_{8-11} and 100 fmol for all other plasmids. As previously described [159], one population of cells were transfected with DSP_{1-7} and the other population transfected with DSP_{8-11} and either a plasmid encoding F or plasmids encoding F and G. Six hours post-transfection, cells were resuspended, mixed with a 1:1 ratio, and supplemented with EnduRen live cell luciferase substrate (Invitrogen, Life Technologies, Calsbad, CA) at 34 μg/mL into a 96-well black plate (Corning, NY). Mixed cells were maintained in a 37 °C 5% CO_2 incubator and luciferase activity was quantified using a TopCount NXT (PerkinElmer, Waltham, MA) 20 hours post-transfection for comparing the fusion activity of different F mutants.

To monitor cell surface expression of F and G proteins in transfected 293T cells in the DSP assays, a separate population of transfected cells for each transfection group was suspended in Versene (Life Technologies, Calsbad, CA) and non-specific binding blocked by Fc receptor blocking TruStain (BioLegend, San Diego, CA) for 30 min at 4 °C. For RSV F surface staining, motavizumab (provided by Nancy Ulbrandt, MedImmune, Gaithersburg, MD) and PE-mouse anti-human were used. For RSV G staining, mouse monoclonal anti-RSV G (131-2G, Millipore, MAB858-2) and APC-rat-

anti-mouse were used. All antibodies were used at 1:500 dilutions in a final volume of 100 μL. Gating on F and G positive signals were based on setting the control groups with only the corresponding secondary antibodies at 0.1-0.2%. Cells were analyzed using an LSRII cytometer and FlowJo software (Tree Star, Ashland, OR).

Statistical analysis. Statistical analyses were performed using GraphPad Prism software version 6.0 (San Diego, CA). Data are represented as means with standard errors of the means (SEMs). One-way and two-way analysis of variance (ANOVA) with Tukey's *post hoc* test with a *P* value of 0.05 were used.

RESULTS

Generation of recombinant viruses

Since RSV G attachment protein is produced both as a membrane bound form as well as a secreted form due to an alternative translation initiation site, we mutated both methionines to isoleucine [35] and changed the second codon in the G open reading frame (ORF) into a premature stop codon to abolish the expression of this gene without grossly perturbing its genome integrity (Fig. 1A). We did not change the codon following the second methionine to abolish the secreted G expression since previous work has shown substituting the second methionine to isoleucine is enough to abolish secreted G [35]. As expected, Western blots of sucrose purified virus stocks showed that both the Gstop viruses (kRSV-GstopA2F and kRSV-Gstop2-20F) expressed no G protein. Interestingly, there are two bands for G protein seen in the virus containing both G and F genes (kRSV-A2G-A2F and kRSV-2-20G-2-20F). The larger band (labeled G-L in Fig. 1B) has a molecular weight (M.W.) of 90-100 kD, consistent with the full-length membrane bound form, whereas the smaller form (labeled G-S in Fig. 1B) has a M.W. close to 50 kD. Although the lower band of G has a similar M.W. to the secreted form of G from the Long strain [39], the identity of this band cannot be ascertained without more detailed analysis. Densitometry analysis of Western blots showed no difference in the F protein abundance in purified virus, consistent with previously published data showing the absence of G did not alter the F protein level in the virions [59]. The virus containing both 2-20 G and 2-20 F proteins has significantly more G-S than virus containing both glycoproteins from the A2 strain.

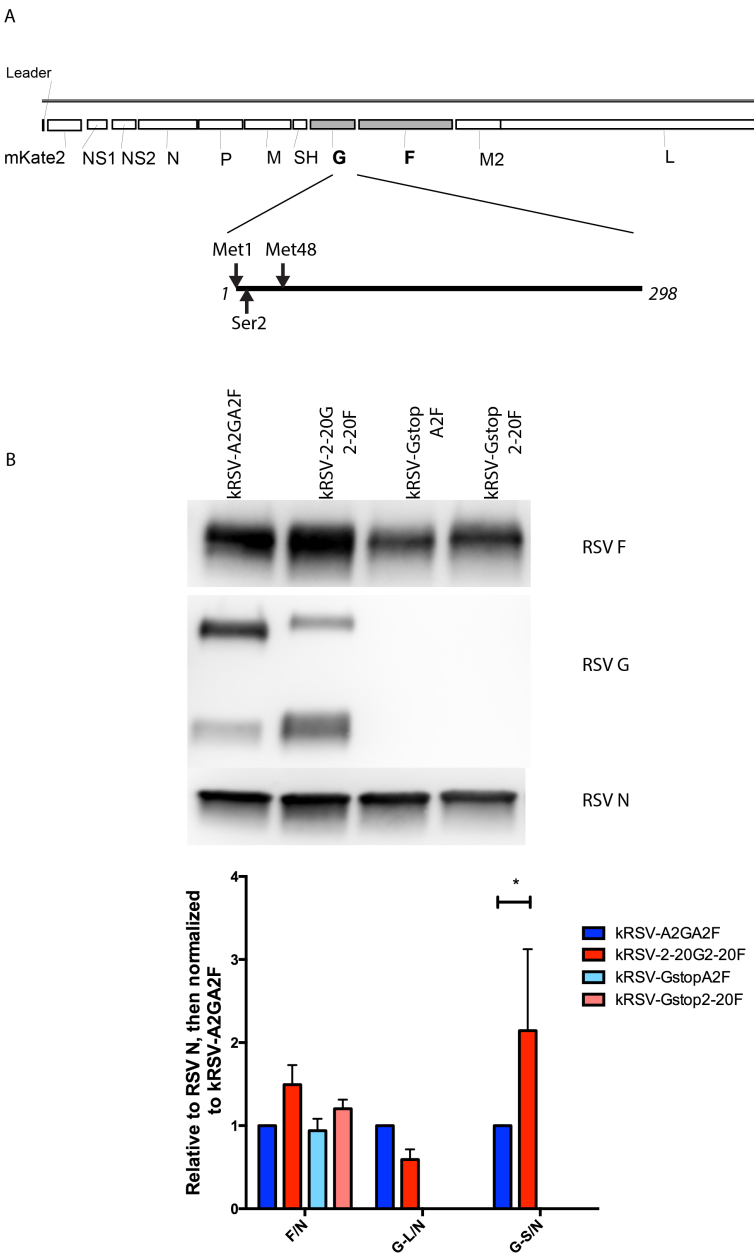

Fig 1. Schematic design of the recombinant viruses and quantification of surface glycoproteins in purified virions.

(A) RSV genome with G gene open reading frame (amino acids 1 to 298) enlarged to illustrate the mutations made to generate the Gstop virus. The two methionines were changed to isoleucine and the second codon (serine) was changed to a stop codon. (B) Western blot showing the F, G, and N protein expression levels (top) and densitometry

from two independent experiments shown at the bottom. * $P < 0.05$ using one-way ANOVA. Data are represented as mean ± SEM.

Differential contribution of G protein to virus attachment to host cells

Since the F protein of the lab-adapted A2 strain has been shown to also bind to the host cells possibly through interactions with heparin sulfate, we then asked whether the G protein from the 2-20 strain contributes to host cell binding activity differently from that of the A2 G [23, 24, 153]. To test this hypothesis, we used sucrose purified virus stocks and normalized the relative amount of virions used as input for this binding assay based on the N protein expression levels by Western blotting. The N protein expression level is shown to correlate well with the radiolabeled activity in the virus preparations [59]. The kRSV-2-20G-2-20F virus bound to BEAS-2B cells almost 3-fold better than the kRSV-A2G-A2F virus (Fig. 2). Removal of the A2 G protein from the virus resulted in loss of at least half of the binding to this cell line (comparing kRSV-GstopA2F to kRSV-A2G-A2F in Fig. 2). However, removal of 2-20 G protein from the virus resulted in more than 90% binding of the virus to the cells (comparing kRSV-Gstop2-20F to kRSV-2-20G-2-20F in Fig. 2). Thus, 2-20 G did contribute to greater binding activity of the virus to the host cell than the A2 G, at least in the BEAS-2B cell line. Our observation that A2 G mediated about 50% of binding is consistent with previously published data [24].

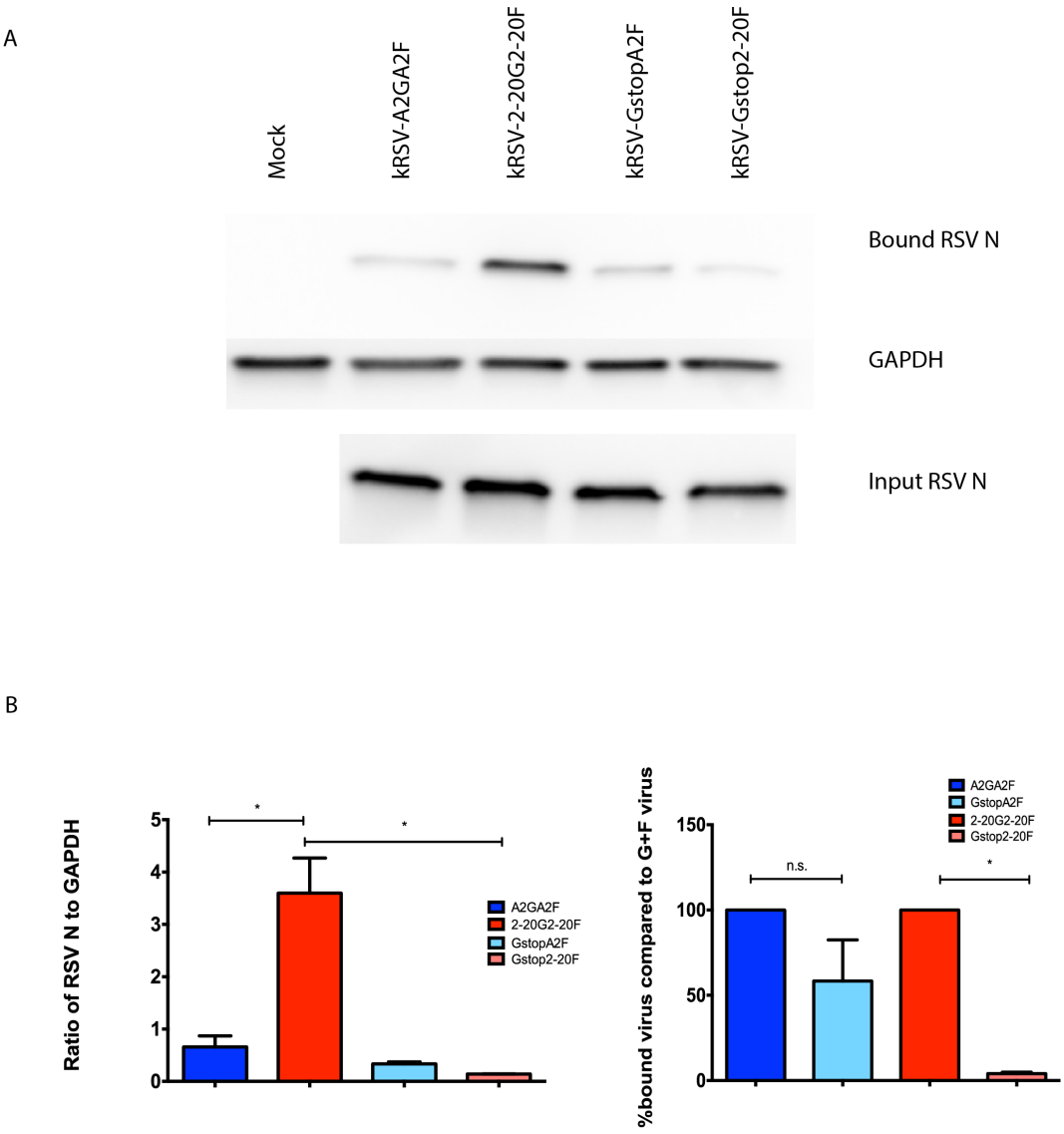

Fig 2. Greater contribution of 2-20 G than A2 G to binding to the cell.

(A) Western blots showing a representative binding assay. Input virus inoculums were normalized based on the N protein expression levels as shown on the bottom blot. (B) Densitometry analysis of bound virus. All raw virus binding activity (B, left) was calculated by normalizing the N protein level (bound RSV N from the top blot) to GAPDH level of the same sample. This value for the Gstop viruses was further normalized to that of its parental virus containing both F and G and represented as

"%bound virus compared to G+F virus" (B. right). * $P < 0.05$. Data are represented as mean ± SEM.

Greater contribution of 2-20 G to virus entry kinetics than A2 G

To further explore the functional differences of 2-20 G compared to A2 G, we tested whether virus entry into the host cell would be differentially affected by the removal of either G protein. We compared the entry kinetics of all four viruses in BEAS-2B cells using a citrate entry assay [156]. kRSV-A2G-A2F virus had the highest entry kinetics, followed by kRSV-GstopA2F virus (Fig. 3A). Removal of A2 G from the virus resulted in a 3-fold decrease in entry efficiency of the virus (Fig. 3B). Interestingly, removal of 2-20 G from the virus decreased the entry kinetics by almost 8-fold (Fig. 3C). Thus, 2-20 G mediated much more entry than A2 G, similar to binding activity shown in Fig. 2. We believe this enhanced entry by the 2-20 G is not entirely due to its enhanced binding activity (see Discussion for explanation).

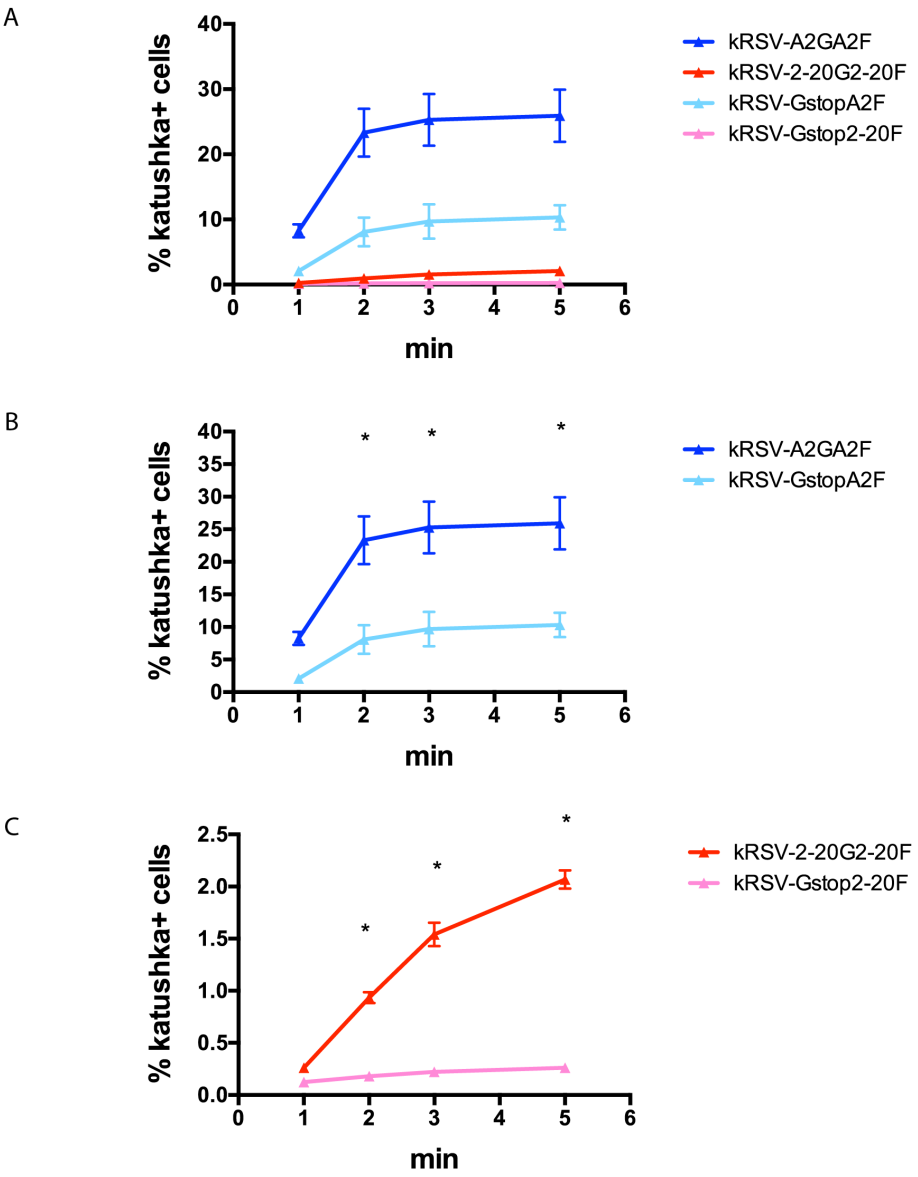

Fig 3. Entry kinetics in BEAS-2B cells.

(A) Overall view of the relative entry kinetics of all four viruses. (B) Contribution of A2 G protein to the entry kinetics of kRSV-A2G-A2F compared to kRSV-GstopA2F. (C) Contribution of 2-20 G protein to the entry kinetics of kRSV-2-20G-2-20F compared to kRSV-Gstop2-20F. * $P < 0.05$. Data are represented as mean ± SEM.

Infectivity in cell lines

Since the 2-20 G contributed much more to both virus binding to the host cells as well as virus entry kinetics than the A2 G, we next examined if the 2-20 G could also affect virus infectivity in various cell lines more than the A2 G. Infectivity of each virus was assayed in three cell lines, BEAS-2B, CHO-K1, and pgsD-677. BEAS-2B is a cell line that represents human bronchial epithelial cells, while CHO-K1 and pgsD-677 were used for comparing the effect of the presence and absence of GAGs (pgsD-677 is a heparin sulfate deficient CHO-K1 derivative). In all these cell lines, the virus containing both glycoproteins had much a higher infectivity than the corresponding virus that lack the G protein. To compare the relative contribution of the G protein to virus infectivity, we normalized the percent of infected cells by the Gstop virus to the percent of infected cells by the virus containing both G and F proteins (kRSV-GstopA2F normalized to kRSV-A2G-A2F and kRSV-Gstp2-20F normalized to kRSV-2-20G2-20F; Fig. 4). In BEAS-2B and CHO-K1 cells (both expressing heparin sulfate), A2 G contributed to 30-40% infectivity whereas 2-20 G contributed to more than 80% (Fig. 4A, B). Moreover, the contribution of 2-20 G protein was evident even in the heparin sulfate deficient pgsD-677 cell line while A2 G no longer had any significant contribution to infection, consistent with the notion that the G protein from lab-adapted strains of RSV mostly binds to GAGs present on the immortalized cell lines (Fig. 4C).

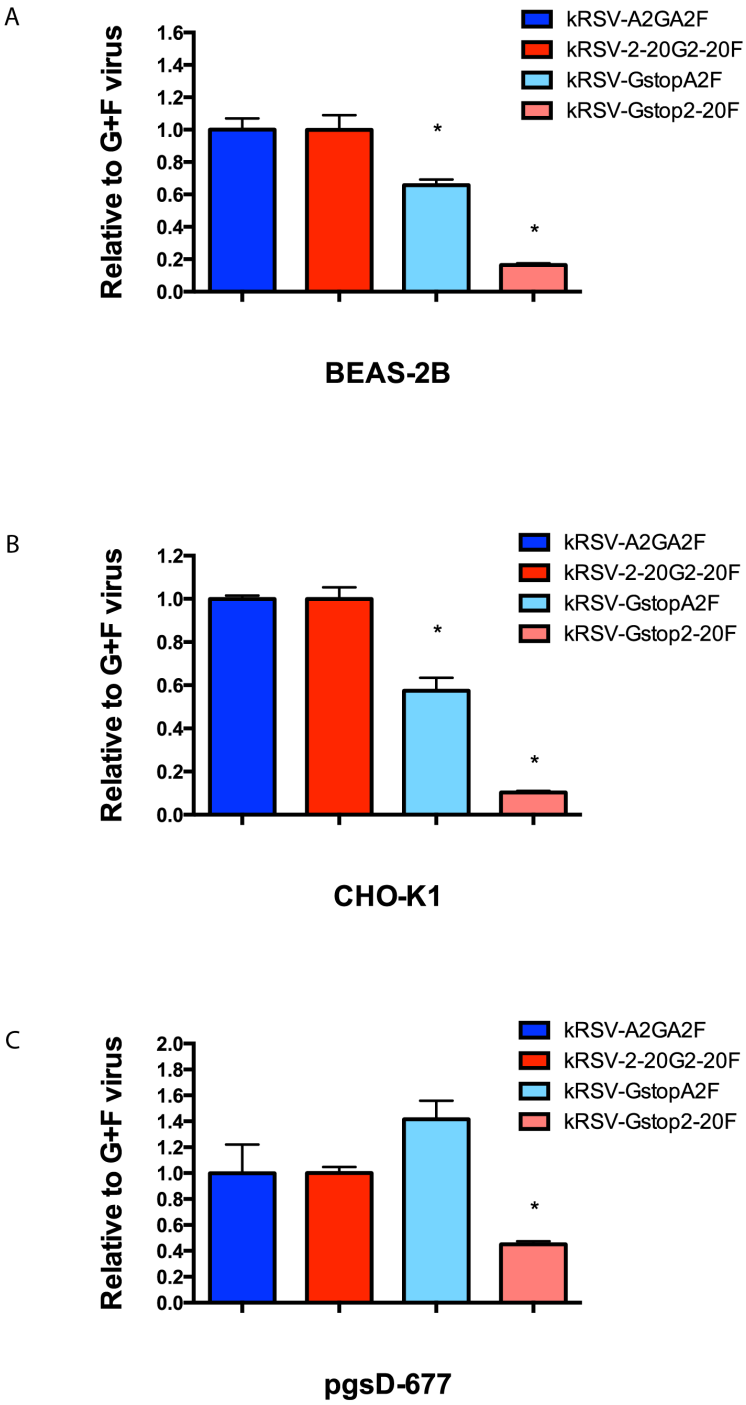

Fig 4. Infectivity in BEAS-2B, CHO-K1, and pgsD-677 cell lines.

Normalized infectivity in BEAS-2B (A), CHO-K1 (B), and pgsD-677 (C) cell lines. * $P < 0.05$ using one-way ANOVA. Data are represented as mean ± SEM.

In vitro Growth kinetics in HEp-2 and BEAS-2B cell lines

Since the 2-20 G protein affected the viral infectivity differentially, we also compared the growth kinetics of all four viruses in both HEp-2 and BEAS-2B cell lines using MOI of 0.01. As reported previously by Teng, *et al*., the absence of G protein from A2 strain did not grossly affect the growth of the virus in HEp-2 cell line (Fig. 5A) [35]. The original of the G and F glycoprotein did not affect the growth of the virus as kRSV-A2G-A2F and RSV-2-20G-2-20F grew to similar levels in both cell lines (Fig. 5A). However, the absence of 2-20 G from the virus greatly affected its growth in HEp-2 and more dramatically, in BEAS-2B cell line (Fig. 5B). Compared to kRSV-2-20G-2-20F virus, kRSV-Gstop2-20F virus had a consistently more than 2 $\log_{10}$ drop in titer in BEAS-2B cell line.

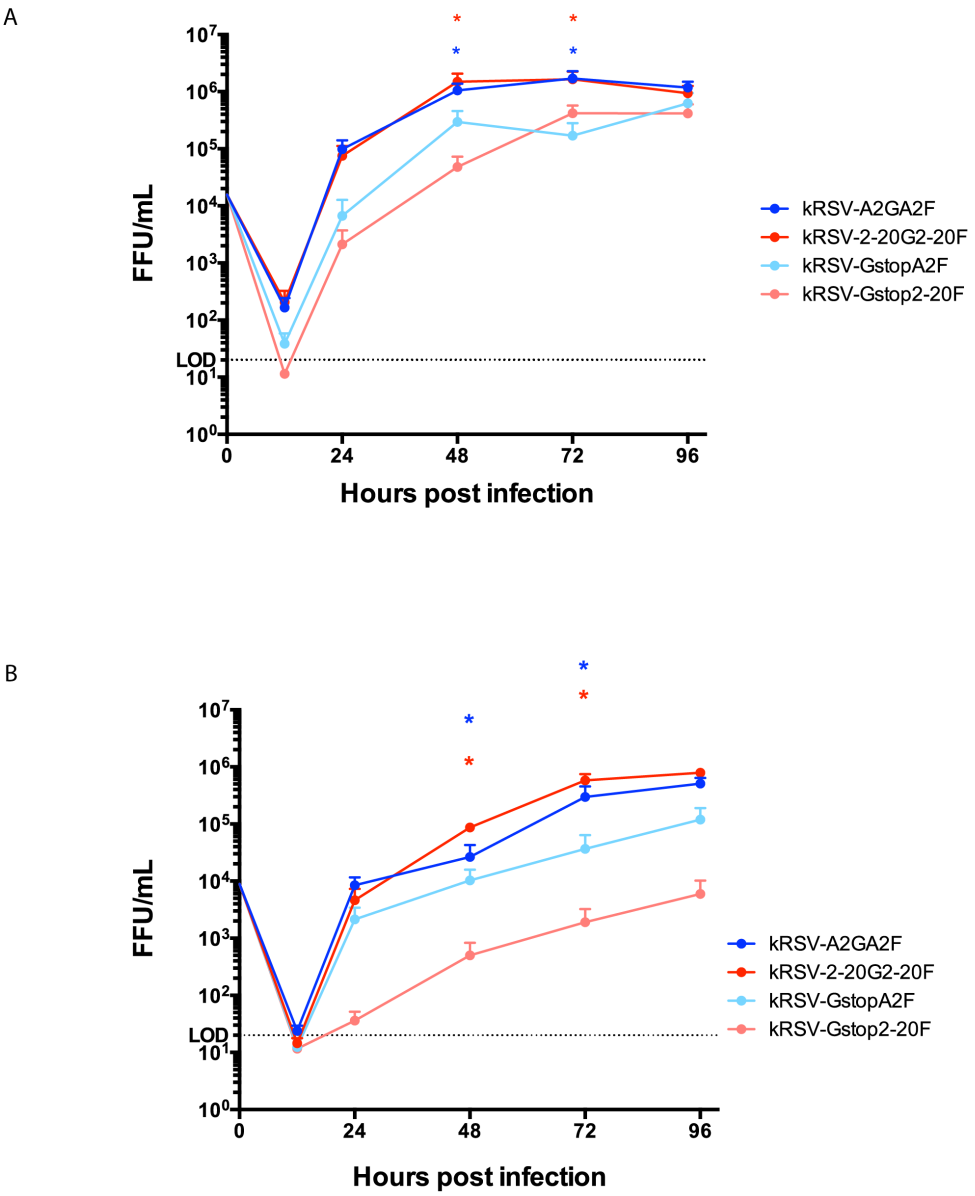

Fig 5. Contribution of G protein to virus *in vitro* growth kinetics.

HEp-2 cell line (A) and BEAS-2B cell line (B) were infected with either kRSV-A2G-A2F, kRSV-2-20G-2-20F, kRSV-GstopA2F, or kRSV-Gstop2-20F virus using an MOI of 0.01. Virus titers at each time point were assayed by FFU assay. * $P < 0.05$. Data are represented as mean ± SEM. LOD, limit of detection. FFU, fluorescent focus unit.

Differential contribution of G protein to F-mediated cell-cell fusion

Lastly, we compared the fusion activity of the F protein in the presence or absence of the G protein in a cell-to-cell fusion assay. Previous study using A2 F and A2 G expressed from a vaccinia virus system showed that the A2 G protein can enhance cell-to-cell fusion of A2 F protein, presumably through enhancing cell-to-cell attachment [59]. However, we did not see the same result when A2 F and A2 G were co-transfected into the same cells. But the fusion boost was seen only with the 2-20 F and 2-20 G co-expressed, and this fusion boost was restricted to the homologous combination of G and F for the 2-20 strain, since the 2-20 G did not boost the fusion activity of the A2 F, nor did the A2 G boost the fusion activity of the 2-20 F (Fig. 6A). Moreover, we have mapped a domain (amino acids 101-156) in the 2-20 G and amino acid 63 on the 2-20 F that are associated with this fusion boost, suggesting the possibility that this enhancement of 2-20 F fusion by the 2-20 G protein could be due to factors other than enhancing the attachment to the host cells. The amino acids 101-156 in the 2-20 G was associated with 2-20 F fusion boost since the mutant A2 G with this region cloned from the 2-20 G (A2Gm in Fig. 6A) still maintained the ability to boost the 2-20 F fusion activity, but not that of the A2 F (Fig. 6A). Sequence comparison between the A2 F and 2-20 F revealed six amino acids (amino acids 63, 66, 76, 384, 519, 524) most likely involved in the fusion boost based on published RSV F structure. The corresponding 2-20 F mutants with either one or several of these sites mutated back to the amino acids of A2 F were generated and tested for the fusion activity in DSP assay. Most of the mutants had very low fusion activity except for the 2-20 F_63, which had a higher fusion activity by itself but completely abolished the fusion boost by the 2-20 G (Fig. 6B), indicating this site is very important in mediating interaction with 2-20 G for its fusion boost activity.

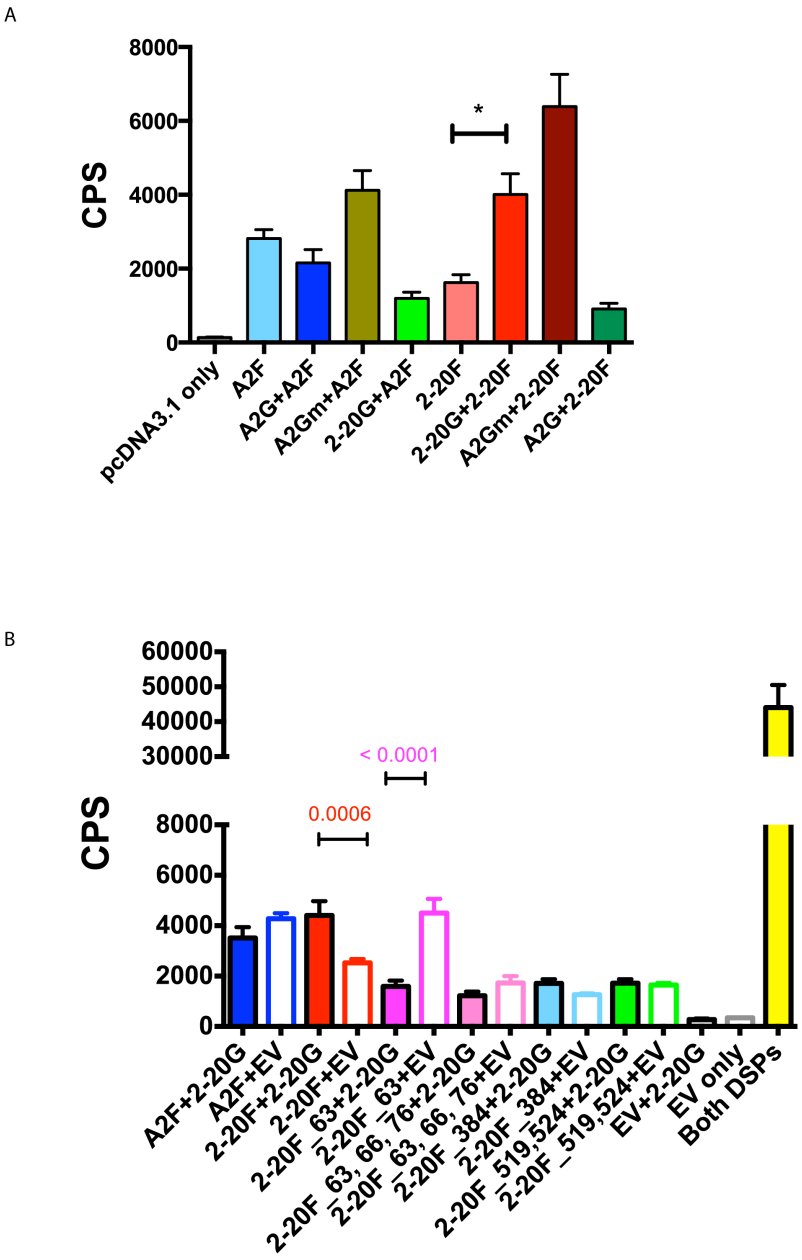

Fig 6. Cell-to-cell fusion activity by dual-split protein fusion assay.

(A) 2-20 G boosts fusion activity of 2-20 F, which is mediated by the region encompassing amino acids 101-156. (B) Mapping amino acid 63 on 2-20 F associated with fusion boost. * $P < 0.05$. Data are represented as mean ± SEM. EV, empty vector pcDNA3.1.

DISCUSSION

RSV is classified into two antigenic subgroups A and B based on the variable G gene extracellular domain sequence. There is some evidence suggesting RSV strain differences contribute to different pathological outcomes [62, 69, 72, 73]. Several studies using different clinical isolates of RSV compared to the prototypic A2 strain invariably demonstrated that the clinical strains can be more virulent in well differentiated cell culture systems or in animal models [62, 72, 73]. Thus, reevaluating the important gene functions for clinical isolates of RSV is important for better understanding the pathogenesis of this virus. Interestingly, the strain used in this study has been shown to induce more severe disease in the BALB/c mouse model [73], thus making it interesting to explore whether this different contributions of the G attachment protein can be extended to other RSV clinical isolates and whether these functional differences may be contributing to different disease outcomes. The results from these further studies can also guide vaccine design and antiviral drug development.

In this study, we have compared the functions of RSV attachment protein G from a clinical isolate, A2001/2-20, to that of the most commonly used lab-adapted strain A2, including attachment, fusion enhancement, entry kinetics, infectivity and growth kinetics. Overall, the attachment protein from this clinical isolate had exhibited greater contributions in all of the above functions involved in RSV infection, especially in the early phase of infection. To our knowledge, this is the first study to reevaluate the contribution of the attachment protein for this virus using a clinical isolate strain and revealed some functional differences between a lab-adapted strain and a clinical isolate.

Previous studies analyzing the attachment protein G functions all used lab-adapted strains such as A2 and Long [35, 59], or a strain that has been passaged extensively *in vitro* [11]. Exclusive use of *in vitro* culture adapted strains for virus research can have the potential to overlook some functions that get lost during extensive passaging and selection in cell cultures. Using these culture adapted strains, lack of G attachment protein from the virus does not grossly affect virus replication *in vitro*, thus making G a dispensable protein for RSV. Related animal virus, BRSV, the attachment protein G is also shown to be dispensable for efficient *in vitro* growth [58]. Out findings with one particular clinical isolate of RSV suggest some functional difference exist between the non-adapted clinical isolate and the lab-adapted strain, and more similar studies with other clinical isolates should be done.

This is thus far the first study demonstrating the functional interaction between the RSV glycoproteins, attachment G protein and the fusion F protein, in promoting fusion. Previous studies using only the lab-adapted strains of RSV (A2 and Long) were unable to detect this functional interaction. Whether RSV glycoprotein pairs function more like the Newcastle disease virus (NDV) in an association model or more like the Measles virus (MeV) in a dissociation model needs further studies [160]. Domain 101-156 in the 2-20 G mediated fusion-enhancing specificity for its homologous F, much like the stalk domain of other *Paramyxovirus* H or HN in determining the F specificity. Because there is no crystal structure for RSV G protein available, it is hard to define whether this domain (101-156 aa) is indeed located in the stalk region. Also, slightly

different is that this region in 2-20 G is associated with enhancing fusion activity of homologous F, not F triggering *per se*. So there might be some fundamental different mechanisms in RSV G attachment protein function in fusion process than from other members of the *Paramyxovirus*. Other clinical isolates of RSV should be tested for this fusion enhancing activity and if this should be a general phenomenon for RSV clinical isolates, this fusion enhancing domain should constitute a novel attractive target for antiviral drugs, which could not be revealed by using lab-adapted strains.

Although many members of the *Paramyxovirus* have a strict requirement for the attachment protein (NH or H) to trigger fusion, such as NDV and MeV, there are some known exceptions in this virus family. Sendai virus fusion protein has been shown to bypass the requirement for its attachment protein HN in infecting cells with ASGP-R surface expression, although the presence of HN can enhance infectivity [161]. The fusion protein of simian virus 5 (SV5) has also been shown to induce membrane fusion independent of the abundance of its HN protein, which is thought to only provide binding activity necessary for optimal distance between the fusion protein and cellular target(s) [162]. Likewise, the attachment protein G of RSV has been thought to simply facilitate fusion enhancement by bringing the two membranes into close proximity [150]. This hypothesis is not consistent with our observations since the G protein has to be expressed with its homotypic F protein for the fusion boost. Furthermore, we also have a F mutant (2-20 F_63) that completely abolished the G dependency for fusion boost, thus making it conceivable that for RSV strain 2-20, G provides functions other than binding to the target cell *per se*. Other viral surface glycoproteins have also been shown to enhance

membrane fusion, such as Influenza virus neuraminidase (NA), possibly through deasilyation of the viral HA [163].

We hypothesized based on the functional differences between the clinical isolate G protein and the lab-adapted strain, that certain mutations in either the F or G, or both, could arise during serial passages and cell culture adaptation of RSV. This has been noted for a variety of *Paramyxovirus*, even for NDV, the fusion protein of which has a very stringent requirement for its HN protein, there have been reports that certain amino acid changes in the F1 domain can completely abolish this requirement [164, 165]. It is possible that similar mutations can happen in RSV strains during serial passages in tissue cultures, thus somehow changing the requirement for RSV attachment protein's function in promoting fusion. What would be the selective advantage for this type of mutations for RSV in cell cultures is currently unknown.

ACKNOWLEDGMENTS

This work was supported by NIH grants 1R01AI087798 and 1U19AI095227, and funds from the Children's Center for Immunology and Vaccines (CCIV).

We thank Nancy Ulbrandt (MedImmune LLC) for the motavizumab mAb. We thank Ursula Buchholz and Karl-Klaus Conzelmann for the BSR-T7/5 cells. We thank Naoyuki Kondo and Zene Matsuda for the DSP_{1-7} and DSP_{8-11} plasmids used in the DSP assay. We thank the Emory Children's Pediatric Research Center flow cytometry core supported by Children's Healthcare of Atlanta.

CHAPTER 4: DISCUSSION

Respiratory syncytial virus (RSV) still represents an unmet medical challenge for which no vaccines or specific antivirals are approved, despite decades of efforts on developing effective treatment regimens against this ubiquitous virus. Currently, there is only a prophylactic humanized monoclonal antibody against the RSV fusion protein (F), palivizumab, but it is only prescribed for infants with underlying risk factors (prematurity, congenital heart diseases, congenital lung dysplasia) while the majority of infants developing severe RSV bronchiolitis and pneumonia are without such risk factors. Failure of the 1960s formalin-inactivated RSV vaccine trial further emphasized the importance of understanding the mechanisms of pathogenesis and developing effective methods for attenuating the virus for vaccine purpose.

Major obstacles that hinder the development of an effective RSV vaccine include: 1) initial RSV infection occurs very early in age while the respiratory and immune systems in infants are still undergoing development; 2) RSV can effectively evade innate immunity and does not induce a strong protective adaptive immunity, thus allowing reinfection to occur without major antigenic changes in the virus; 3) small animal models of RSV disease do not recapitulate all aspects of critical features of human disease; 4) the legacy of vaccine-enhanced illness associated with formalin-inactivated RSV trial (reviewed in [119]). Among the various RSV vaccine target populations, infants younger than 6 months of age are considered the highest priority target for RSV vaccines since peak occurrence for severe RSV illness occurs within this age group. For safety concerns, live-attenuated vaccine is currently the major type of vaccine for this target population, a population considered at risk for vaccine-enhanced disease [166]. In older children,

adults (mostly pregnant mothers) and elderly, subunit and particle-based vaccines are the most commonly explored strategies.

Commonly used methods for attenuating RSV, or almost any virus, include using chemical mutagens, growing virus in sub-optimal hosts or tissue cultures, or under sub-optimal temperatures to introduce mutations that adapt the virus to replicate well under these specific conditions but not so well when reintroduced into the original hosts. With the establishment of reverse genetics systems for a particular virus, gene deletions, modifications, or gene swapping are also emerging as effective methods for virus attenuation [167]. Targeting viral replicative fitness may predetermine the difficulty of maintaining the immunogenicity of live-attenuated vaccines. This is particularly the case for RSV vaccine development as wild-type virus is relatively virulent, especially for RSV-naïve infants, but not very immunogenic, thus making it desirable to attenuate the virus with minimal reduction in its immunogenicity. The majority of the RSV live-attenuated vaccine candidates were not attenuated to the right level for RSV sero-negative infants, thus not advancing past phase I clinical trials [55, 118]. Of the limited number of live-attenuated RSV vaccine candidates that did advance into clinical trials (MEDI-559), reversions and compensatory mutations make further safety testing a requirement [110].

In order to attenuate RSV to an appropriate level without causing subsequent reversions or compensatory mutations, we attempted the codon deoptimization approach on this virus and selectively targeted the two nonstructural (NS) genes out of a total of ten

genes in the viral genome. We chose NS1 and NS2 genes as our targets based on their biological functions during a productive RSV infection, which include suppression of host innate immune responses by targeting type I and type III IFN pathways in both the epithelial cells and immune cells, suppressing the host adaptive immune responses and skewing the Th responses, and delaying apoptosis and activating host pro-inflammatory pathways (NF-κB) [81, 85-92, 94]. Our goal was to generate an attenuated vaccine candidate with close to wild-type replicative fitness *in vitro* for large-scale production but that replicated poorly at least in small animal models such as BALB/c mouse. We have achieved this by greatly reducing, but not abolishing, the expression of both NS1 and NS2 genes (Chapter 2 Fig. 3) so that the recoded virus was still capable to replicate similarly to the wild-type virus in Vero cells (Chapter 2 Fig. 4B), but not in the BALB/c mouse model (Chapter 2 Fig. 5A). Our NS1/NS2 codon deoptimized virus differed from the NS1//NS2 deletion virus in *in vitro* replication fitness and we attributed this to residual NS1 and NS2 activities that could counteract the antiviral responses in Vero cells (not type I IFN response) [90].

We also speculated that codon deoptimized NS1 and NS2 would contribute to enhanced host innate responses to the virus (mainly type I/III IFN responses) and possibly also enhanced adaptive responses previously suppressed by the abundant NS1 and NS2 proteins expressed early during RSV infection. In several studies using NS1/NS2 deletion virus, type I/III IFN responses are higher when NS1 and NS2 proteins are absent during infection [88, 90]. We did not compare the IFN protein levels from cell lines that were infected with either virus but did try to quantify the type I IFN and type III

IFN from infected BALB/c mice lungs and BAL. In these experiments, there was no significant difference between the wild-type and the codon deoptimized virus (data not shown). Generally, the levels of both type I and type III IFNs from infected BALB/c mice measured by ELISA were quite low (close to the limit of detection of the kits). Given that the NS1/NS2 codon deoptimized virus was attenuated by a $\log_{10}$ FFU in this mouse model (Chapter 2 Fig. 5A), we speculate that it did induced more IFN on a per virion basis, was more sensitive to IFN responses, or both. An alternative to directly quantifying the IFN protein levels in infected mice is to measure the various interferon-stimulated genes (ISGs) by real-time PCR. We are currently exploring this aspect using primary human bronchial epithelial cells (NHBE) differentiated at air-liquid interface, infected with wild-type virus, the NS1/NS2 genes codon deoptimized virus, or mock infected. We will compare the transcriptional profile of genes, especially those involved in IFN response pathways and that have antiviral activities (data in progress).

Some studies also suggest RSV NS1 and NS2 proteins can target human STAT2 more efficiently than the mouse STAT2 [88] and if that is true, our NS1/NS2 codon deoptimized virus would be more attenuated in humans and may also be more immunogenic than our mouse data suggested (Chapter 2 Fig. 5B-D). This is in line with our data that the greatest reduction in NS1/NS2 codon deoptimized virus replication was seen in NHBE cells (Chapter 2 Fig. 4D-F).

Besides their well characterized roles in antiviral innate immunity, type I IFNs can also promote adaptive immunity, including the antibody response mediated by B

cells (reviewed in [168]). This could explain our observation that NS1/NS2 codon deoptimized virus infection in BALB/c mice induced higher levels of RSV neutralizing antibody than the parental virus, despite a 10-fold reduced replication (antigen load) in the mouse model (Chapter 2 Fig. 4 and 5). This further substantiates our rationale for targeting the viral immune suppressive genes in order to attenuate the virus with minimal reduction in its immunogenicity.

To our knowledge, this is the first time the viral immune suppressive genes were targeted through reduced expression (codon deoptimization) to achieve a proper level of attenuation while maintaining immunogenicity. This novel method of attenuation added a useful component to the development of live-attenuated RSV vaccine candidates with improved genetics stability (Chapter 2).

Like NS1 and NS2 genes, the G attachment glycoprotein of RSV is also defined as a nonessential gene for virus replication *in vitro*, but its absence can attenuate viral growth more *in vivo*. A great number of studies have analyzed the effect of removing the G protein from the virus on infection, replication, and pathogenesis. It is understandable that due to the lack of reverse genetics systems for clinical isolates, most of these studies have had to rely on using the A2 strain for functional studies. However, we speculated that clinical isolates of RSV represented more closely the virus biology, and thus we decided to re-assess the functions of G protein, although still using the A2-based reverse genetics system, in the context of its homologous F protein. We believe this could recapitulate some features of the RSV clinical isolates, since G and F are the major

glycoproteins on the virion surface. Very recently, a similar reverse genetics system for a clinical RSV B strain was developed and this could provide more insights into the G protein function during early RSV infection [54].

Another modification we made in the current study in the design of the G-null mutant virus is that, instead of deleting the entire ORF for the G gene, we only used point mutations to abrogate the expression of G protein without compromising the genome structure. This is due to the concern that deleting a gene from a paramyxovirus genome could shift the entire transcription gradient downstream of the gene being deleted, further complicating the functional studies. All previous studies on RSV G gene functions are based on G deletion viruses.

The G protein of the clinical strain A2001/2-20 did have several functional differences when compared to the G protein of the lab-adapted strain A2. In all aspects of the functions analyzed in the current study, 2-20 G exhibited a much greater contribution to each step of RSV infection, binding to the host cells (Chapter 3 Fig. 2), virus entry into the host cells (Chapter 3 Fig. 3), *in vitro* infectivity in both GAG-competent as well as GAG-deficient cell lines (Chapter 3 Fig. 4), and virus replication in immortalized cell lines (Chapter 3 Fig. 5). Most interestingly, the 2-20 G protein demonstrated a novel function not shared with A2 G by modulating the fusion activity of its homologous F protein in a cell-to-cell fusion assay (Chapter 3 Fig. 6). We believe this F-specific fusion boost activity of G is not entirely the result of increased binding of the virus to the host cell (see next two paragraphs).

We also tried to map the relevant domains and important amino acid sites on both 2-20 G and 2-20 F associated with this fusion boost phenotype. After sequence comparison between the A2 G and 2-20 G, we identified a region encompassing amino acids 101 to 156 that contains most of differences. Therefore, we generated a mutant A2 G with this region replaced by the sequence from the 2-20 G (A2 Gm in Chapter 3 Fig. 6A). This region conferred the A2 G the capability to boost the fusion activity of 2-20 F, but not A2 F, similar to the 2-20 G protein (Chapter 3 Fig. 6A). This region lies in the first mucin-like region of RSV G, thus should contain potential glycosylation sites and be highly glycosylated [151]. Whether the glycans in the G protein could affect the fusion boost phenotype is not explored here.

We also compared the sequences of A2 F and 2-20 F and found a total of six amino acids most likely involved in the fusion process. These are amino acids 63, 66, 76, 384, 519, and 524. The first three residues, 63, 66, and 76 cluster at the head domain in the RSV F pre-fusion structure, and two residues (63 and 66) are part of the newly discovered antigenic site Φ [20]. This antigenic site is not preserved in the post-fusion F structure, suggesting large-scale rearrangement during the fusion process. Interestingly, when only amino acid 63 was mutated on 2-20 F (threonine changed to asparagine), fusion activity of F protein alone increased (Chapter 3 Fig. 6B). But when all three sites were changed back to amino acids from A2 F, fusion activity of F mutant decreased dramatically (Chapter 3 Fig. 6B). Amino acid changes at residues 384 (located in α8, membrane-proximal lobe, and not undergoing dramatic rearrangement during fusion),

519 and 524 (in close proximity to the membrane) also drastically decreased the F fusion activity. Therefore, except for residue 63, we cannot conclude whether these sites are important in mediating interaction with 2-20 G for boosting fusion due to the intrinsic minimal fusion activity of these 2-20 F mutants. However, for 2-20 F_63 mutant with increased fusion activity in the absence of the 2-20 G, addition of 2-20 G actually inhibited the fusion activity (Chapter 3 Fig. 6B). This observation led us to argue against the hypothesis that 2-20 G boosts 2-20 F fusion simply by providing binding to the host cell. If the above hypothesis holds true, for 2-20 F_63 mutant, the fusion activity should not be affected, if not increased, by the 2-20 G, which was not what we observed. Therefore, residue 63 on 2-20 F could be mediating interaction with 2-20 G, underlying the fusion boost only with the homologous F and G for the 2-20 strain.

Previous studies have identified 15 potential heparin-binding domains (HBD) in the A2 F protein using heparin-binding chromatography [23]. Compared to the six amino acid residues different between the A2 F and 2-20 F, only residues 63, 66, and 76 are located in two overlapping HBDs. Although this may explain decreased binding to the host cell by kRSV-Gstop2-20F than the kRSV-GstopA2F, neither of which contained the G glycoprotein (Chapter 3 Fig. 2B), peptides corresponding to neither HBD can inhibit virus binding to the cells or infectivity [23]. Use of different cell lines (Vero in [23] and BEAS-B in this study) could be an explanation for this discrepancy. One way to test this could be to test the inhibitory effect of corresponding peptides in BEAS-2B cells.

Our current observations regarding the G protein functions for clinical RSV isolates are novel, suggesting additional RSV clinical isolates should also be evaluated. We compared the A2 F sequence with additional clinical isolates, including the 2-20 strain, and found residues 66, 76, 384, and 519 are conserved in the clinical isolates, different from those in A2 (Fig. 1).

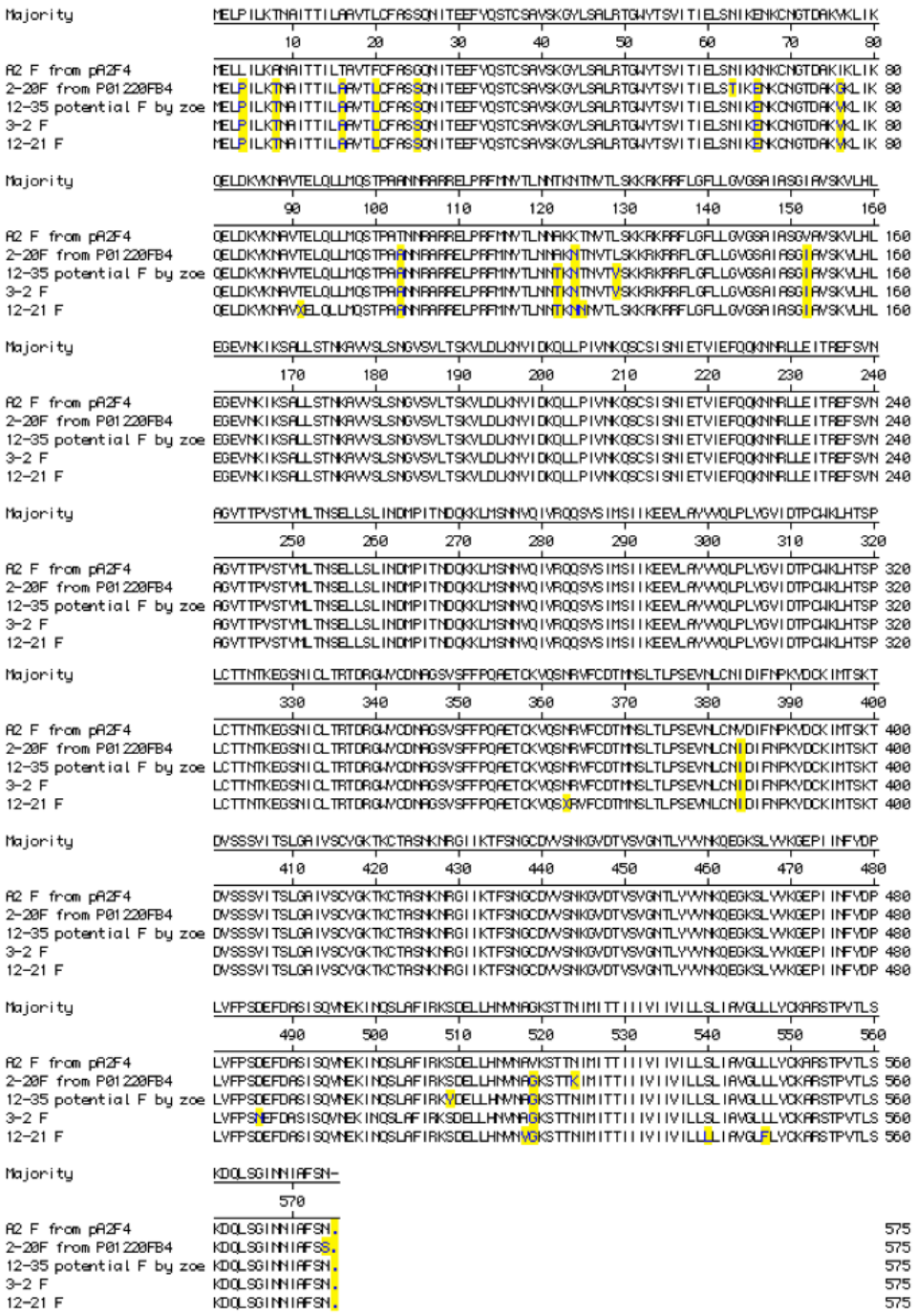

Fig 1. F protein sequence comparison of A2 strain with several clinical isolates.

Sequences were aligned using the MegaAlign module in DNAStar Lasergene software. Yellow boxes indicate the residues different from that of A2 F. The consensus sequence is at the top of the alignment.

In conclusion, we explored the various methods of attenuating RSV by mutating its nonessential genes (NS1, NS2, and G) and found several interesting observations. First, reducing but not abolishing the expression of RSV virulence genes with immune suppressive functions (NS1 and NS2) could be a novel mechanism for virus attenuation with retained immunogenicity. Coupled with the codon deoptimization method, the attenuated virus could be genetically stable, and therefore become novel attenuating modules for developing RSV live-attenuated vaccine candidates. Second, the functional contribution of RSV nonessential gene (G glycoprotein) can be strain-dependent. This is revealed by using the A2001/2-20 strain G protein and analyzing phenotypic differences due to its absence from the virion. Collectively, the data indicated the G protein from this strain had a greater contribution to virus infection (binding, entry, and fusion) and replication *in vitro*. The above information should all be included into consideration when designing RSV live-attenuated vaccines in the future.

REFERENCE

1. Nair, H., et al., *Global burden of acute lower respiratory infections due to respiratory syncytial virus in young children: a systematic review and meta-analysis*. Lancet, 2010. **375**(9725): p. 1545-55.
2. Stockman, L.J., et al., *Respiratory syncytial virus-associated hospitalizations among infants and young children in the United States, 1997-2006*. Pediatr Infect Dis J, 2012. **31**(1): p. 5-9.
3. Zhou, H., et al., *Hospitalizations associated with influenza and respiratory syncytial virus in the United States, 1993-2008*. Clin Infect Dis, 2012. **54**(10): p. 1427-36.
4. Jain, S., et al., *Community-acquired pneumonia requiring hospitalization among U.S. children*. N Engl J Med, 2015. **372**(9): p. 835-45.
5. Walsh, E.E., *Respiratory syncytial virus infection in adults*. Semin Respir Crit Care Med, 2011. **32**(4): p. 423-32.
6. Langley, G.F. and L.J. Anderson, *Epidemiology and prevention of respiratory syncytial virus infections among infants and young children*. Pediatr Infect Dis J, 2011. **30**(6): p. 510-7.
7. Collins, P.L. and J. James E. Crowe, *Respiratory Syncytial Virus and Metapneumovirus*, in *Field's Virology*. 2006, Lippincott Williams & Wilkins.
8. Cui, G., et al., *Genetic variation in attachment glycoprotein genes of human respiratory syncytial virus subgroups a and B in children in recent five consecutive years*. PLoS One, 2013. **8**(9): p. e75020.

9. Liljeroos, L., et al., *Architecture of respiratory syncytial virus revealed by electron cryotomography*. Proc Natl Acad Sci U S A, 2013. **110**(27): p. 11133-8.

10. Kiss, G., et al., *Structural analysis of respiratory syncytial virus reveals the position of M2-1 between the matrix protein and the ribonucleoprotein complex*. J Virol, 2014. **88**(13): p. 7602-17.

11. Karron, R.A., et al., *Respiratory syncytial virus (RSV) SH and G proteins are not essential for viral replication in vitro: clinical evaluation and molecular characterization of a cold-passaged, attenuated RSV subgroup B mutant*. Proc Natl Acad Sci U S A, 1997. **94**(25): p. 13961-6.

12. Gan, S.W., et al., *The small hydrophobic protein of the human respiratory syncytial virus forms pentameric ion channels*. J Biol Chem, 2012. **287**(29): p. 24671-89.

13. Fuentes, S., et al., *Function of the respiratory syncytial virus small hydrophobic protein*. J Virol, 2007. **81**(15): p. 8361-6.

14. Collins, P.L., Y.T. Huang, and G.W. Wertz, *Nucleotide sequence of the gene encoding the fusion (F) glycoprotein of human respiratory syncytial virus*. Proc Natl Acad Sci U S A, 1984. **81**(24): p. 7683-7.

15. Collins, P.L. and G. Mottet, *Post-translational processing and oligomerization of the fusion glycoprotein of human respiratory syncytial virus*. J Gen Virol, 1991. **72 (Pt 12)**: p. 3095-101.

16. Begona Ruiz-Arguello, M., et al., *Effect of proteolytic processing at two distinct sites on shape and aggregation of an anchorless fusion protein of human*

respiratory syncytial virus and fate of the intervening segment. Virology, 2002. **298**(2): p. 317-26.

17. Rixon, H.W., et al., *Multiple glycosylated forms of the respiratory syncytial virus fusion protein are expressed in virus-infected cells*. J Gen Virol, 2002. **83**(Pt 1): p. 61-6.
18. Gonzalez-Reyes, L., et al., *Cleavage of the human respiratory syncytial virus fusion protein at two distinct sites is required for activation of membrane fusion*. Proc Natl Acad Sci U S A, 2001. **98**(17): p. 9859-64.
19. Swanson, K.A., et al., *Structural basis for immunization with postfusion respiratory syncytial virus fusion F glycoprotein (RSV F) to elicit high neutralizing antibody titers*. Proc Natl Acad Sci U S A, 2011. **108**(23): p. 9619-24.
20. McLellan, J.S., et al., *Structure of RSV fusion glycoprotein trimer bound to a prefusion-specific neutralizing antibody*. Science, 2013. **340**(6136): p. 1113-7.
21. McLellan, J.S., et al., *Structure of respiratory syncytial virus fusion glycoprotein in the postfusion conformation reveals preservation of neutralizing epitopes*. J Virol, 2011. **85**(15): p. 7788-96.
22. Kahn, J.S., et al., *Recombinant vesicular stomatitis virus expressing respiratory syncytial virus (RSV) glycoproteins: RSV fusion protein can mediate infection and cell fusion*. Virology, 1999. **254**(1): p. 81-91.
23. Crim, R.L., et al., *Identification of linear heparin-binding peptides derived from human respiratory syncytial virus fusion glycoprotein that inhibit infectivity*. J Virol, 2007. **81**(1): p. 261-71.

24. Techaarpornkul, S., P.L. Collins, and M.E. Peeples, *Respiratory syncytial virus with the fusion protein as its only viral glycoprotein is less dependent on cellular glycosaminoglycans for attachment than complete virus*. Virology, 2002. **294**(2): p. 296-304.

25. Tayyari, F., et al., *Identification of nucleolin as a cellular receptor for human respiratory syncytial virus*. Nat Med, 2011. **17**(9): p. 1132-5.

26. Behera, A.K., et al., *Blocking intercellular adhesion molecule-1 on human epithelial cells decreases respiratory syncytial virus infection*. Biochem Biophys Res Commun, 2001. **280**(1): p. 188-95.

27. Malhotra, R., et al., *Isolation and characterisation of potential respiratory syncytial virus receptor(s) on epithelial cells*. Microbes Infect, 2003. **5**(2): p. 123-33.

28. Tripp, R.A., et al., *CX3C chemokine mimicry by respiratory syncytial virus G glycoprotein*. Nat Immunol, 2001. **2**(8): p. 732-8.

29. Kurt-Jones, E.A., et al., *Pattern recognition receptors TLR4 and CD14 mediate response to respiratory syncytial virus*. Nat Immunol, 2000. **1**(5): p. 398-401.

30. Collins, P.L. and G. Mottet, *Oligomerization and post-translational processing of glycoprotein G of human respiratory syncytial virus: altered O-glycosylation in the presence of brefeldin A*. J Gen Virol, 1992. **73 (Pt 4)**: p. 849-63.

31. Garcia-Beato, R., et al., *Host cell effect upon glycosylation and antigenicity of human respiratory syncytial virus G glycoprotein*. Virology, 1996. **221**(2): p. 301-9.

32. Kwilas, S., et al., *Respiratory syncytial virus grown in Vero cells contains a truncated attachment protein that alters its infectivity and dependence on glycosaminoglycans*. J Virol, 2009. **83**(20): p. 10710-8.

33. Teng, M.N. and P.L. Collins, *The central conserved cystine noose of the attachment G protein of human respiratory syncytial virus is not required for efficient viral infection in vitro or in vivo*. J Virol, 2002. **76**(12): p. 6164-71.

34. Feldman, S.A., R.M. Hendry, and J.A. Beeler, *Identification of a linear heparin binding domain for human respiratory syncytial virus attachment glycoprotein G*. J Virol, 1999. **73**(8): p. 6610-7.

35. Teng, M.N., S.S. Whitehead, and P.L. Collins, *Contribution of the respiratory syncytial virus G glycoprotein and its secreted and membrane-bound forms to virus replication in vitro and in vivo*. Virology, 2001. **289**(2): p. 283-96.

36. Harcourt, J., et al., *Respiratory syncytial virus G protein and G protein CX3C motif adversely affect CX3CR1+ T cell responses*. J Immunol, 2006. **176**(3): p. 1600-8.

37. Trento, A., et al., *Major changes in the G protein of human respiratory syncytial virus isolates introduced by a duplication of 60 nucleotides*. J Gen Virol, 2003. **84**(Pt 11): p. 3115-20.

38. Eshaghi, A., et al., *Genetic variability of human respiratory syncytial virus A strains circulating in Ontario: a novel genotype with a 72 nucleotide G gene duplication*. PLoS One, 2012. **7**(3): p. e32807.

39. Hendricks, D.A., et al., *Appearance of a soluble form of the G protein of respiratory syncytial virus in fluids of infected cells*. J Gen Virol, 1987. **68 (Pt 6)**: p. 1705-14.

40. Hendricks, D.A., K. McIntosh, and J.L. Patterson, *Further characterization of the soluble form of the G glycoprotein of respiratory syncytial virus*. J Virol, 1988. **62**(7): p. 2228-33.

41. Roberts, S.R., et al., *The membrane-associated and secreted forms of the respiratory syncytial virus attachment glycoprotein G are synthesized from alternative initiation codons*. J Virol, 1994. **68**(7): p. 4538-46.

42. Escribano-Romero, E., et al., *The soluble form of human respiratory syncytial virus attachment protein differs from the membrane-bound form in its oligomeric state but is still capable of binding to cell surface proteoglycans*. J Virol, 2004. **78**(7): p. 3524-32.

43. Bukreyev, A., L. Yang, and P.L. Collins, *The secreted G protein of human respiratory syncytial virus antagonizes antibody-mediated restriction of replication involving macrophages and complement*. J Virol, 2012. **86**(19): p. 10880-4.

44. Bukreyev, A., et al., *The secreted form of respiratory syncytial virus G glycoprotein helps the virus evade antibody-mediated restriction of replication by acting as an antigen decoy and through effects on Fc receptor-bearing leukocytes*. J Virol, 2008. **82**(24): p. 12191-204.

45. Hardy, R.W. and G.W. Wertz, *The product of the respiratory syncytial virus M2 gene ORF1 enhances readthrough of intergenic junctions during viral transcription*. J Virol, 1998. **72**(1): p. 520-6.

46. Grosfeld, H., M.G. Hill, and P.L. Collins, *RNA replication by respiratory syncytial virus (RSV) is directed by the N, P, and L proteins; transcription also occurs under these conditions but requires RSV superinfection for efficient synthesis of full-length mRNA*. J Virol, 1995. **69**(9): p. 5677-86.

47. Collins, P.L., et al., *Transcription elongation factor of respiratory syncytial virus, a nonsegmented negative-strand RNA virus*. Proc Natl Acad Sci U S A, 1996. **93**(1): p. 81-5.

48. Collins, P.L., et al., *Production of infectious human respiratory syncytial virus from cloned cDNA confirms an essential role for the transcription elongation factor from the 5' proximal open reading frame of the M2 mRNA in gene expression and provides a capability for vaccine development*. Proc Natl Acad Sci U S A, 1995. **92**(25): p. 11563-7.

49. Hanley, L.L., et al., *Roles of the respiratory syncytial virus trailer region: effects of mutations on genome production and stress granule formation*. Virology, 2010. **406**(2): p. 241-52.

50. Fearns, R., M.E. Peeples, and P.L. Collins, *Mapping the transcription and replication promoters of respiratory syncytial virus*. J Virol, 2002. **76**(4): p. 1663-72.

51. Bermingham, A. and P.L. Collins, *The M2-2 protein of human respiratory syncytial virus is a regulatory factor involved in the balance between RNA*

replication and transcription. Proc Natl Acad Sci U S A, 1999. **96**(20): p. 11259-64.

52. Wei, T., et al., *The eukaryotic elongation factor 1A is critical for genome replication of the paramyxovirus respiratory syncytial virus*. PLoS One, 2014. **9**(12): p. e114447.

53. Hotard, A.L., et al., *A stabilized respiratory syncytial virus reverse genetics system amenable to recombination-mediated mutagenesis*. Virology, 2012. **434**(1): p. 129-36.

54. Lemon, K., et al., *Recombinant subgroup B human respiratory syncytial virus expressing enhanced green fluorescent protein efficiently replicates in primary human cells and is virulent in cotton rats*. J Virol, 2015. **89**(5): p. 2849-56.

55. Collins, P.L. and B.R. Murphy, *New generation live vaccines against human respiratory syncytial virus designed by reverse genetics*. Proc Am Thorac Soc, 2005. **2**(2): p. 166-73.

56. Meng, J., et al., *Refining the balance of attenuation and immunogenicity of respiratory syncytial virus by targeted codon deoptimization of virulence genes*. MBio, 2014. **5**(5): p. e01704-14.

57. Whitehead, S.S., et al., *Replacement of the F and G proteins of respiratory syncytial virus (RSV) subgroup A with those of subgroup B generates chimeric live attenuated RSV subgroup B vaccine candidates*. J Virol, 1999. **73**(12): p. 9773-80.

58. Karger, A., U. Schmidt, and U.J. Buchholz, *Recombinant bovine respiratory syncytial virus with deletions of the G or SH genes: G and F proteins bind heparin*. J Gen Virol, 2001. **82**(Pt 3): p. 631-40.

59. Techaarpornkul, S., N. Barretto, and M.E. Peeples, *Functional analysis of recombinant respiratory syncytial virus deletion mutants lacking the small hydrophobic and/or attachment glycoprotein gene*. J Virol, 2001. **75**(15): p. 6825-34.

60. Zhang, L., et al., *Respiratory syncytial virus infection of human airway epithelial cells is polarized, specific to ciliated cells, and without obvious cytopathology*. J Virol, 2002. **76**(11): p. 5654-66.

61. Guo-Parke, H., et al., *Relative respiratory syncytial virus cytopathogenesis in upper and lower respiratory tract epithelium*. Am J Respir Crit Care Med, 2013. **188**(7): p. 842-51.

62. Villenave, R., et al., *In vitro modeling of respiratory syncytial virus infection of pediatric bronchial epithelium, the primary target of infection in vivo*. Proc Natl Acad Sci U S A, 2012. **109**(13): p. 5040-5.

63. Wright, P.F., et al., *Growth of respiratory syncytial virus in primary epithelial cells from the human respiratory tract*. J Virol, 2005. **79**(13): p. 8651-4.

64. Burnham, A.J., et al., *Competitive fitness of influenza B viruses with neuraminidase inhibitor-resistant substitutions in a coinfection model of the human airway epithelium*. J Virol, 2015. **89**(8): p. 4575-87.

65. Elbahesh, H., et al., *Novel roles of focal adhesion kinase in cytoplasmic entry and replication of influenza A viruses*. J Virol, 2014. **88**(12): p. 6714-28.

66. Escaffre, O., et al., *Henipavirus pathogenesis in human respiratory epithelial cells*. J Virol, 2013. **87**(6): p. 3284-94.

67. Ilyushina, N.A., et al., *Human-like receptor specificity does not affect the neuraminidase-inhibitor susceptibility of H5N1 influenza viruses*. PLoS Pathog, 2008. **4**(4): p. e1000043.

68. Peret, T.C., et al., *Circulation patterns of genetically distinct group A and B strains of human respiratory syncytial virus in a community*. J Gen Virol, 1998. **79 (Pt 9)**: p. 2221-9.

69. Melero, J.A. and M.L. Moore, *Influence of respiratory syncytial virus strain differences on pathogenesis and immunity*. Curr Top Microbiol Immunol, 2013. **372**: p. 59-82.

70. Levitz, R., et al., *Induction of IL-6 and CCL5 (RANTES) in human respiratory epithelial (A549) cells by clinical isolates of respiratory syncytial virus is strain specific*. Virol J, 2012. **9**: p. 190.

71. Villenave, R., et al., *Differential cytopathogenesis of respiratory syncytial virus prototypic and clinical isolates in primary pediatric bronchial epithelial cells*. Virol J, 2011. **8**: p. 43.

72. Derscheid, R.J., et al., *Human respiratory syncytial virus memphis 37 causes acute respiratory disease in perinatal lamb lung*. Biores Open Access, 2014. **3**(2): p. 60-9.

73. Stokes, K.L., et al., *Differential pathogenesis of respiratory syncytial virus clinical isolates in BALB/c mice*. J Virol, 2011. **85**(12): p. 5782-93.

74. Liu, P., et al., *Retinoic acid-inducible gene I mediates early antiviral response and Toll-like receptor 3 expression in respiratory syncytial virus-infected airway epithelial cells*. J Virol, 2007. **81**(3): p. 1401-11.

75. Rudd, B.D., et al., *Differential role for TLR3 in respiratory syncytial virus-induced chemokine expression*. J Virol, 2005. **79**(6): p. 3350-7.

76. Murawski, M.R., et al., *Respiratory syncytial virus activates innate immunity through Toll-like receptor 2*. J Virol, 2009. **83**(3): p. 1492-500.

77. Rudd, B.D., et al., *Deletion of TLR3 alters the pulmonary immune environment and mucus production during respiratory syncytial virus infection*. J Immunol, 2006. **176**(3): p. 1937-42.

78. Haeberle, H.A., et al., *Respiratory syncytial virus-induced activation of nuclear factor-kappaB in the lung involves alveolar macrophages and toll-like receptor 4-dependent pathways*. J Infect Dis, 2002. **186**(9): p. 1199-206.

79. Monick, M.M., et al., *Respiratory syncytial virus up-regulates TLR4 and sensitizes airway epithelial cells to endotoxin*. J Biol Chem, 2003. **278**(52): p. 53035-44.

80. Groskreutz, D.J., et al., *Respiratory syncytial virus induces TLR3 protein and protein kinase R, leading to increased double-stranded RNA responsiveness in airway epithelial cells*. J Immunol, 2006. **176**(3): p. 1733-40.

81. Schlender, J., et al., *Inhibition of toll-like receptor 7- and 9-mediated alpha/beta interferon production in human plasmacytoid dendritic cells by respiratory syncytial virus and measles virus*. J Virol, 2005. **79**(9): p. 5507-15.

82. Lukacs, N.W., et al., *Respiratory virus-induced TLR7 activation controls IL-17-associated increased mucus via IL-23 regulation*. J Immunol, 2010. **185**(4): p. 2231-9.

83. Demoor, T., et al., *IPS-1 signaling has a nonredundant role in mediating antiviral responses and the clearance of respiratory syncytial virus*. J Immunol, 2012. **189**(12): p. 5942-53.

84. Elliott, J., et al., *Respiratory syncytial virus NS1 protein degrades STAT2 by using the Elongin-Cullin E3 ligase*. J Virol, 2007. **81**(7): p. 3428-36.

85. Goswami, R., et al., *Viral degradasome hijacks mitochondria to suppress innate immunity*. Cell Res, 2013. **23**(8): p. 1025-42.

86. Hastie, M.L., et al., *The human respiratory syncytial virus nonstructural protein 1 regulates type I and type II interferon pathways*. Mol Cell Proteomics, 2012. **11**(5): p. 108-27.

87. Ling, Z., K.C. Tran, and M.N. Teng, *Human respiratory syncytial virus nonstructural protein NS2 antagonizes the activation of beta interferon transcription by interacting with RIG-I*. J Virol, 2009. **83**(8): p. 3734-42.

88. Lo, M.S., R.M. Brazas, and M.J. Holtzman, *Respiratory syncytial virus nonstructural proteins NS1 and NS2 mediate inhibition of Stat2 expression and alpha/beta interferon responsiveness*. J Virol, 2005. **79**(14): p. 9315-9.

89. Ramaswamy, M., et al., *Respiratory syncytial virus nonstructural protein 2 specifically inhibits type I interferon signal transduction*. Virology, 2006. **344**(2): p. 328-39.

90. Spann, K.M., et al., *Suppression of the induction of alpha, beta, and lambda interferons by the NS1 and NS2 proteins of human respiratory syncytial virus in human epithelial cells and macrophages [corrected]*. J Virol, 2004. **78**(8): p. 4363-9.

91. Spann, K.M., K.C. Tran, and P.L. Collins, *Effects of nonstructural proteins NS1 and NS2 of human respiratory syncytial virus on interferon regulatory factor 3, NF-kappaB, and proinflammatory cytokines*. J Virol, 2005. **79**(9): p. 5353-62.

92. Swedan, S., A. Musiyenko, and S. Barik, *Respiratory syncytial virus nonstructural proteins decrease levels of multiple members of the cellular interferon pathways*. J Virol, 2009. **83**(19): p. 9682-93.

93. Xu, X., et al., *Respiratory syncytial virus NS1 protein degrades STAT2 by inducing SOCS1 expression*. Intervirology, 2014. **57**(2): p. 65-73.

94. Bitko, V., et al., *Nonstructural proteins of respiratory syncytial virus suppress premature apoptosis by an NF-kappaB-dependent, interferon-independent mechanism and facilitate virus growth*. J Virol, 2007. **81**(4): p. 1786-95.

95. Jin, H., et al., *Evaluation of recombinant respiratory syncytial virus gene deletion mutants in African green monkeys for their potential as live attenuated vaccine candidates*. Vaccine, 2003. **21**(25-26): p. 3647-52.

96. Jin, H., et al., *Recombinant respiratory syncytial viruses with deletions in the NS1, NS2, SH, and M2-2 genes are attenuated in vitro and in vivo*. Virology, 2000. **273**(1): p. 210-8.

97. Teng, M.N., et al., *Recombinant respiratory syncytial virus that does not express the NS1 or M2-2 protein is highly attenuated and immunogenic in chimpanzees*. J Virol, 2000. **74**(19): p. 9317-21.

98. Whitehead, S.S., et al., *Recombinant respiratory syncytial virus bearing a deletion of either the NS2 or SH gene is attenuated in chimpanzees*. J Virol, 1999. **73**(4): p. 3438-42.

99. Mazumder, B., et al., *Extraribosomal l13a is a specific innate immune factor for antiviral defense*. J Virol, 2014. **88**(16): p. 9100-10.

100. Kotelkin, A., et al., *The NS2 protein of human respiratory syncytial virus suppresses the cytotoxic T-cell response as a consequence of suppressing the type I interferon response*. J Virol, 2006. **80**(12): p. 5958-67.

101. Munir, S., et al., *Respiratory syncytial virus interferon antagonist NS1 protein suppresses and skews the human T lymphocyte response*. PLoS Pathog, 2011. **7**(4): p. e1001336.

102. Munir, S., et al., *Nonstructural proteins 1 and 2 of respiratory syncytial virus suppress maturation of human dendritic cells*. J Virol, 2008. **82**(17): p. 8780-96.

103. Zhang, W., et al., *Vaccination to induce antibodies blocking the CX3C-CX3CR1 interaction of respiratory syncytial virus G protein reduces pulmonary inflammation and virus replication in mice*. J Virol, 2010. **84**(2): p. 1148-57.

104. Chirkova, T., et al., *Respiratory syncytial virus G protein CX3C motif impairs human airway epithelial and immune cell responses*. J Virol, 2013. **87**(24): p. 13466-79.

105. Cespedes, P.F., et al., *Surface expression of the hRSV nucleoprotein impairs immunological synapse formation with T cells*. Proc Natl Acad Sci U S A, 2014. **111**(31): p. E3214-23.

106. Jahnz-Rozyk, K., *[Health economic impact of viral respiratory infections and pneumonia diseases on the elderly population in Poland]*. Pol Merkur Lekarski, 2010. **29**(169): p. 37-40.

107. Guvenel, A.K., C. Chiu, and P.J. Openshaw, *Current concepts and progress in RSV vaccine development*. Expert Rev Vaccines, 2014. **13**(3): p. 333-44.

108. Jorquera, P.A., K.E. Oakley, and R.A. Tripp, *Advances in and the potential of vaccines for respiratory syncytial virus*. Expert Rev Respir Med, 2013. **7**(4): p. 411-27.

109. Kim, H.W., et al., *Respiratory syncytial virus disease in infants despite prior administration of antigenic inactivated vaccine*. Am J Epidemiol, 1969. **89**(4): p. 422-34.

110. Malkin, E., et al., *Safety and immunogenicity of a live attenuated RSV vaccine in healthy RSV-seronegative children 5 to 24 months of age*. PLoS One, 2013. **8**(10): p. e77104.

111. Wright, P.F., et al., *The absence of enhanced disease with wild type respiratory syncytial virus infection occurring after receipt of live, attenuated, respiratory syncytial virus vaccines*. Vaccine, 2007. **25**(42): p. 7372-8.

112. Delgado, M.F., et al., *Lack of antibody affinity maturation due to poor Toll-like receptor stimulation leads to enhanced respiratory syncytial virus disease*. Nat Med, 2009. **15**(1): p. 34-41.

113. Schickli, J.H., J. Kaur, and R.S. Tang, *Nonclinical phenotypic and genotypic analyses of a Phase 1 pediatric respiratory syncytial virus vaccine candidate MEDI-559 (rA2cp248/404/1030DeltaSH) at permissive and non-permissive temperatures*. Virus Res, 2012. **169**(1): p. 38-47.

114. Ventre, K. and A. Randolph, *Ribavirin for respiratory syncytial virus infection of the lower respiratory tract in infants and young children*. Cochrane Database Syst Rev, 2004(4): p. CD000181.

115. *Palivizumab, a humanized respiratory syncytial virus monoclonal antibody, reduces hospitalization from respiratory syncytial virus infection in high-risk infants. The IMpact-RSV Study Group*. Pediatrics, 1998. **102**(3 Pt 1): p. 531-7.

116. Krilov, L.R., *Respiratory syncytial virus disease: update on treatment and prevention*. Expert Rev Anti Infect Ther, 2011. **9**(1): p. 27-32.

117. Hall, C.B., et al., *Respiratory syncytial virus-associated hospitalizations among children less than 24 months of age*. Pediatrics, 2013. **132**(2): p. e341-8.

118. Collins, P.L. and J.A. Melero, *Progress in understanding and controlling respiratory syncytial virus: still crazy after all these years*. Virus Res, 2011. **162**(1-2): p. 80-99.

119. Graham, B.S., *Biological challenges and technological opportunities for respiratory syncytial virus vaccine development*. Immunol Rev, 2011. **239**(1): p. 149-66.

120. Luongo, C., et al., *Respiratory syncytial virus modified by deletions of the NS2 gene and amino acid S1313 of the L polymerase protein is a temperature-*

sensitive, live-attenuated vaccine candidate that is phenotypically stable at physiological temperature. J Virol, 2013. **87**(4): p. 1985-96.

121. Teng, M.N., *The non-structural proteins of RSV: targeting interferon antagonists for vaccine development*. Infect Disord Drug Targets, 2012. **12**(2): p. 129-37.

122. Lin, Y.H., et al., *Genetic stability determinants of temperature sensitive, live attenuated respiratory syncytial virus vaccine candidates*. Virus Res, 2006. **115**(1): p. 9-15.

123. Crowe, J.E., Jr., et al., *Cold-passaged, temperature-sensitive mutants of human respiratory syncytial virus (RSV) are highly attenuated, immunogenic, and protective in seronegative chimpanzees, even when RSV antibodies are infused shortly before immunization*. Vaccine, 1995. **13**(9): p. 847-55.

124. Burns, C.C., et al., *Modulation of poliovirus replicative fitness in HeLa cells by deoptimization of synonymous codon usage in the capsid region*. J Virol, 2006. **80**(7): p. 3259-72.

125. Mueller, S., et al., *Reduction of the rate of poliovirus protein synthesis through large-scale codon deoptimization causes attenuation of viral virulence by lowering specific infectivity*. J Virol, 2006. **80**(19): p. 9687-96.

126. Coleman, J.R., et al., *Virus attenuation by genome-scale changes in codon pair bias*. Science, 2008. **320**(5884): p. 1784-7.

127. Nakamura, Y., T. Gojobori, and T. Ikemura, *Codon usage tabulated from international DNA sequence databases: status for the year 2000*. Nucleic Acids Res, 2000. **28**(1): p. 292.

128. Heinze, B., et al., *Both nonstructural proteins NS1 and NS2 of pneumonia virus of mice are inhibitors of the interferon type I and type III responses in vivo*. J Virol, 2011. **85**(9): p. 4071-84.

129. Bossert, B., S. Marozin, and K.K. Conzelmann, *Nonstructural proteins NS1 and NS2 of bovine respiratory syncytial virus block activation of interferon regulatory factor 3*. J Virol, 2003. **77**(16): p. 8661-8.

130. Valarcher, J.F., et al., *Role of alpha/beta interferons in the attenuation and immunogenicity of recombinant bovine respiratory syncytial viruses lacking NS proteins*. J Virol, 2003. **77**(15): p. 8426-39.

131. Schlender, J., et al., *Bovine respiratory syncytial virus nonstructural proteins NS1 and NS2 cooperatively antagonize alpha/beta interferon-induced antiviral response*. J Virol, 2000. **74**(18): p. 8234-42.

132. Swedan, S., et al., *Multiple functional domains and complexes of the two nonstructural proteins of human respiratory syncytial virus contribute to interferon suppression and cellular location*. J Virol, 2011. **85**(19): p. 10090-100.

133. Teng, M.N. and P.L. Collins, *Altered growth characteristics of recombinant respiratory syncytial viruses which do not produce NS2 protein*. J Virol, 1999. **73**(1): p. 466-73.

134. Vitiello, M., et al., *NF-kappaB as a potential therapeutic target in microbial diseases*. Mol Biosyst, 2012. **8**(4): p. 1108-20.

135. Mueller, S., et al., *Live attenuated influenza virus vaccines by computer-aided rational design*. Nat Biotechnol, 2010. **28**(7): p. 723-6.

136. Yang, C., et al., *Deliberate reduction of hemagglutinin and neuraminidase expression of influenza virus leads to an ultraprotective live vaccine in mice*. Proc Natl Acad Sci U S A, 2013. **110**(23): p. 9481-6.

137. Hershberg, R. and D.A. Petrov, *Selection on codon bias*. Annu Rev Genet, 2008. **42**: p. 287-99.

138. Ikemura, T., *Codon usage and tRNA content in unicellular and multicellular organisms*. Mol Biol Evol, 1985. **2**(1): p. 13-34.

139. Najafabadi, H.S., H. Goodarzi, and R. Salavati, *Universal function-specificity of codon usage*. Nucleic Acids Res, 2009. **37**(21): p. 7014-23.

140. Tuller, T., et al., *An evolutionarily conserved mechanism for controlling the efficiency of protein translation*. Cell, 2010. **141**(2): p. 344-54.

141. Qian, W., et al., *Balanced codon usage optimizes eukaryotic translational efficiency*. PLoS Genet, 2012. **8**(3): p. e1002603.

142. Zhou, M., et al., *Non-optimal codon usage affects expression, structure and function of clock protein FRQ*. Nature, 2013. **495**(7439): p. 111-5.

143. Pechmann, S. and J. Frydman, *Evolutionary conservation of codon optimality reveals hidden signatures of cotranslational folding*. Nat Struct Mol Biol, 2013. **20**(2): p. 237-43.

144. Falsey, A.R. and E.E. Walsh, *Respiratory syncytial virus infection in elderly adults*. Drugs Aging, 2005. **22**(7): p. 577-87.

145. Falsey, A.R., et al., *Respiratory syncytial virus infection in elderly and high-risk adults*. N Engl J Med, 2005. **352**(17): p. 1749-59.

146. DeVincenzo, J.P., et al., *Oral GS-5806 activity in a respiratory syncytial virus challenge study*. N Engl J Med, 2014. **371**(8): p. 711-22.

147. Mackman, R.L., et al., *Discovery of an Oral Respiratory Syncytial Virus (RSV) Fusion Inhibitor (GS-5806) and Clinical Proof of Concept in a Human RSV Challenge Study*. J Med Chem, 2015. **58**(4): p. 1630-43.

148. Wang, G., et al., *Discovery of 4'-Chloromethyl-2'-deoxy-3',5'-di-O-isobutyryl-2'-fluorocytidine (ALS-8176), A First-in-Class RSV Polymerase Inhibitor for Treatment of Human Respiratory Syncytial Virus Infection*. J Med Chem, 2015. **58**(4): p. 1862-78.

149. Plattet, P. and R.K. Plemper, *Envelope protein dynamics in paramyxovirus entry*. MBio, 2013. **4**(4).

150. Chang, A. and R.E. Dutch, *Paramyxovirus fusion and entry: multiple paths to a common end*. Viruses, 2012. **4**(4): p. 613-36.

151. McLellan, J.S., W.C. Ray, and M.E. Peeples, *Structure and function of respiratory syncytial virus surface glycoproteins*. Curr Top Microbiol Immunol, 2013. **372**: p. 83-104.

152. Levine, S., R. Klaiber-Franco, and P.R. Paradiso, *Demonstration that glycoprotein G is the attachment protein of respiratory syncytial virus*. J Gen Virol, 1987. **68 (Pt 9)**: p. 2521-4.

153. Feldman, S.A., S. Audet, and J.A. Beeler, *The fusion glycoprotein of human respiratory syncytial virus facilitates virus attachment and infectivity via an interaction with cellular heparan sulfate*. J Virol, 2000. **74**(14): p. 6442-7.

154. Graham, B.S., et al., *Primary respiratory syncytial virus infection in mice*. J Med Virol, 1988. **26**(2): p. 153-62.

155. Boyoglu-Barnum, S., et al., *A respiratory syncytial virus (RSV) anti-G protein F(ab')2 monoclonal antibody suppresses mucous production and breathing effort in RSV rA2-line19F-infected BALB/c mice*. J Virol, 2013. **87**(20): p. 10955-67.

156. White, L.K., et al., *Nonnucleoside inhibitor of measles virus RNA-dependent RNA polymerase complex activity*. Antimicrob Agents Chemother, 2007. **51**(7): p. 2293-303.

157. Hotard, A.L., et al., *Identification of residues in the human respiratory syncytial virus fusion protein that modulate fusion activity and pathogenesis*. J Virol, 2015. **89**(1): p. 512-22.

158. Stokes, K.L., et al., *The respiratory syncytial virus fusion protein and neutrophils mediate the airway mucin response to pathogenic respiratory syncytial virus infection*. J Virol, 2013. **87**(18): p. 10070-82.

159. Ishikawa, H., et al., *Generation of a dual-functional split-reporter protein for monitoring membrane fusion using self-associating split GFP*. Protein Eng Des Sel, 2012. **25**(12): p. 813-20.

160. Plemper, R.K., M.A. Brindley, and R.M. Iorio, *Structural and mechanistic studies of measles virus illuminate paramyxovirus entry*. PLoS Pathog, 2011. **7**(6): p. e1002058.

161. Leyrer, S., et al., *Sendai virus-like particles devoid of haemagglutinin-neuraminidase protein infect cells via the human asialoglycoprotein receptor*. J Gen Virol, 1998. **79 (Pt 4)**: p. 683-7.

162. Dutch, R.E., S.B. Joshi, and R.A. Lamb, *Membrane fusion promoted by increasing surface densities of the paramyxovirus F and HN proteins: comparison of fusion reactions mediated by simian virus 5 F, human parainfluenza virus type 3 F, and influenza virus HA*. J Virol, 1998. **72**(10): p. 7745-53.

163. Su, B., et al., *Enhancement of the influenza A hemagglutinin (HA)-mediated cell-cell fusion and virus entry by the viral neuraminidase (NA)*. PLoS One, 2009. **4**(12): p. e8495.

164. Sergel, T.A., L.W. McGinnes, and T.G. Morrison, *A single amino acid change in the Newcastle disease virus fusion protein alters the requirement for HN protein in fusion*. J Virol, 2000. **74**(11): p. 5101-7.

165. Ayllon, J., E. Villar, and I. Munoz-Barroso, *Mutations in the ectodomain of newcastle disease virus fusion protein confer a hemagglutinin-neuraminidase-independent phenotype*. J Virol, 2010. **84**(2): p. 1066-75.

166. Anderson, L.J., et al., *Strategic priorities for respiratory syncytial virus (RSV) vaccine development*. Vaccine, 2013. **31 Suppl 2**: p. B209-15.

167. Le Bayon, J.C., et al., *Recent developments with live-attenuated recombinant paramyxovirus vaccines*. Rev Med Virol, 2013. **23**(1): p. 15-34.

168. Vazquez, M.I., J. Catalan-Dibene, and A. Zlotnik, *B cells responses and cytokine production are regulated by their immune microenvironment*. Cytokine, 2015.